blotting but not to immunoprecipitate it under this experimental condition. Therefore, the S83 residue in endogenous Lats2 is the primary phosphorylation site *in vivo*. Taken together, we conclude that Aurora-A is the phosphorylating kinase of Lats2 in the M phase because Aurora-A predominately phosphorylates S83 on Lats2 *in vitro* and this site is also phosphorylated *in vivo*.

Lats2 interacts with Aurora-A

Next, we raised a polyclonal rabbit antibody against GST-Aurora-A protein. 293T cells expressing HA-tagged Aurora-A, -B, -C or vector alone were lysed and analysed by Western blotting with either anti-Aurora-A (Fig. 3C, left panel) or anti-HA (right panel) polyclonal antibody. The anti-Aurora-A antibody specifically recognized only HA-Aurora-A but not HA-Aurora-B or HA-Aurora-C. In addition, the anti-Aurora-A antibody also recognized a band corresponding to the endogenous Aurora-A protein in 293T cells and untransfected HeLa S3 cells. Therefore, it appears that the anti-Aurora-A antibody specifically recognizes the Aurora-A protein and does not crossreact with other proteins. Using this antibody, we performed co-immunoprecipitation experiments to know whether Aurora-A and Lats2 interact *in vivo*. As we were unable to confirm the interaction of endogenous Aurora-A with Lats2 by immunoprecipitation assays using anti-Aurora-A or 3D10 antibodies (data not shown), we co-transfected 293T cells with GFP (green fluorescent protein)-Aurora-A and/or 6Myc-Lats2-1-393 (Fig. 3D, lanes 1–3). When we performed immunoprecipitation experiments with each transfected cell extract by using the anti-GFP antibody, we detected 6Myc-Lats2-1-393 in the GFP-Aurora-A immunoprecipitate (Fig. 3D, top panel, lane 6). In reciprocal immunoprecipitation experiments, GFP-Aurora-A was detected in the 6Myc-Lats2-1-393 immunoprecipitate (Fig. 3D, third panel from top, lane 9). This weak interaction between Lats2 and Aurora-A is reminiscent of an unstable complex that is commonly observed between an enzyme and a substrate. These results indicate that Aurora-A interacts with the N-terminus (1–393 amino acids) of Lats2 *in vivo*, which supports the notion that Lats2 is a phosphorylation target of Aurora-A *in vivo*.

Lats2 co-localizes with Aurora-A at the centrosome

If Lats2 is a phosphorylation target of Aurora-A *in vivo*, it is likely that their subcellular distributions are similar during the cell cycle. To test this possibility, we examined whether Lats2 co-localizes with Aurora-A during various cell cycle stages. As the 3D10 antibody, which was raised against the N-terminal portion (amino acids 78–256) of Lats2, could not detect any endogenous Lats2-specific signals, HeLa S3 cells were transiently transfected with GFP-fused full-length human Lats2 or the GFP-vector alone, followed by immunofluorescence staining with anti-Aurora-A antibody (Fig. 4A). GFP-Lats2 was observed as one or two bright spots beside the nucleus in interphase (left panels, i and ii; green). In prophase, these bright spots translocated toward the opposite poles of the cell (left panel, iii). A similar pattern was also observed for Aurora-A, except that Aurora-A was located within the nucleus (middle panels; red). The nuclear localization of Aurora-A was detected with both of the anti-Aurora-A antibodies and we observed no signal with the secondary antibody alone in our experiments (data not shown). Therefore, it is unlikely that the localization of Aurora-A in the nucleus as determined by these two antibodies is as a result of cross-reaction of anti-Aurora-A antibodies. The yellow spots in the merged images indicate that GFP-Lats2 co-localizes with Aurora-A during interphase, prophase and telophase (right panels). However, when the cells enter metaphase, the GFP-Lats2-specific signal was diffusely distributed throughout the cell (left panel, iv), whereas Aurora-A was localized to two predominant bright spots that are reminiscent of the spindle microtubules and the spindle poles. A similar change in subcellular distribution was also observed in the cells expressing the 6Myc-tagged Lats2 construct (Fig. 4B,i and C,i and ii), and the diffuse distribution of Lats2 was also observed during anaphase (Fig. 4B,ii). Interestingly, when cells enter cytokinesis, GFP-Lats2 was observed again as bright spots and the spots were distributed to daughter cells and localized at each pole (Fig. 4A,v), which is suggestive of re-localization to the centrosomes of GFP-Lats2 when the cells enter cytokinesis. Moreover, GFP-Lats2 was also found at the midbody during cytokinesis (Fig. 4A,v). Together with the previous reports that Aurora-A is localized to the interphase and mitotic centrosomes as well as to the spindle poles (Bischoff *et al.* 1998; Zhou *et al.* 1998), these results indicate that Lats2 co-localizes with Aurora-A at the centrosomes during interphase, early prophase and cytokinesis. That Lats2 localizes to centrosomes during interphase was also confirmed by its co-localization with γ-tubulin (Fig. 4C).

The S83 of Lats2 is phosphorylated at the centrosome, the mitotic spindle pole and the midbody

To confirm that S83 on Lats2 is phosphorylated at the centrosomes *in vivo*, the spatial and temporal distributions

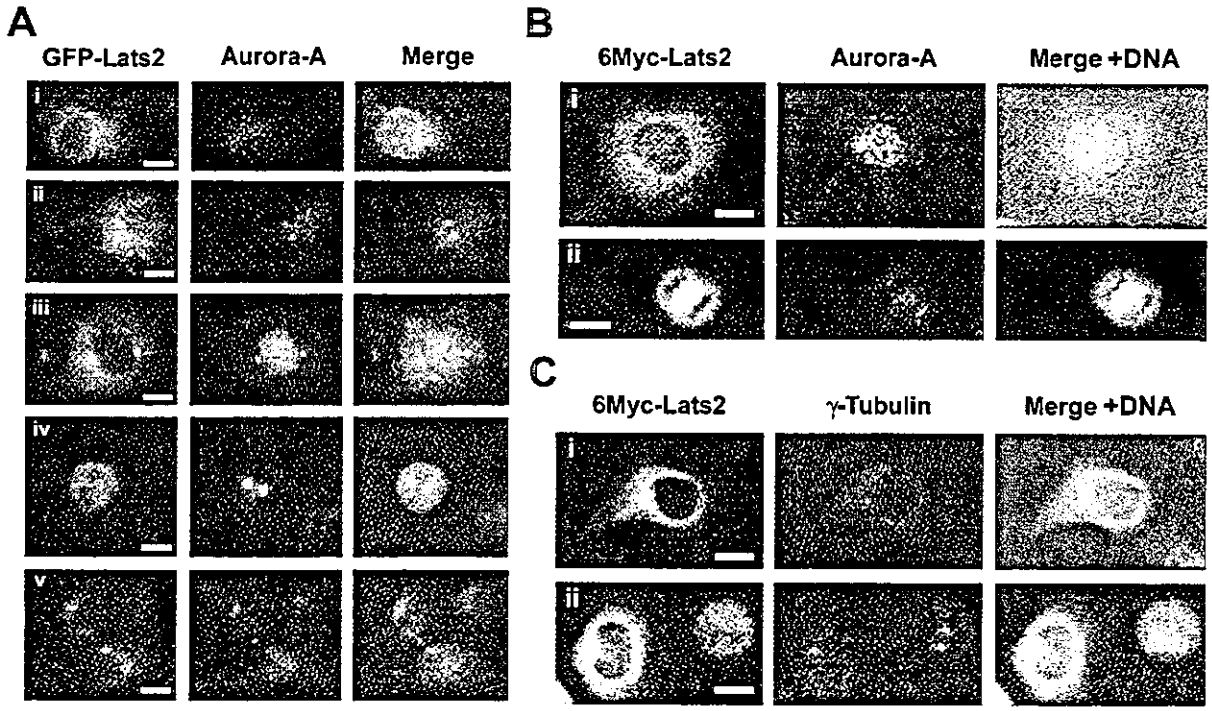

Figure 4 Lats2 co-localizes with Aurora-A at the centrosome. HeLa S3 cells were transiently transfected with GFP-fused full-length Lats2 (A) or 6Myc-tagged full length Lats2 (B and C). The transfected cells were synchronized at the S phase by thymidine-single block, released from the block and then fixed with formaldehyde at various cell cycle stages: interphase (A-i, -ii, B-i and C-i), prophase (A-iii), metaphase (A-iv and C-ii), anaphase (B-ii) and telophase (A-v). 6Myc-Lats2 was visualized by immunofluorescence staining of the fixed cells with anti-Myc antibody followed by incubation with Alexa-Fluor 488-conjugated anti-mouse immunoglobulin G (B and C, green). Aurora-A or centrosomes were visualized by immunofluorescence staining with anti-Aurora-A (A and B, red) or anti-γ tubulin (C, red) antibody, respectively, followed by Texas Red or Alexa-Fluor 594-conjugated anti-rabbit immunoglobulin G. DNA was visualized by staining with Hoechst 33258 (B and C, blue). DNA and merged images are shown in the right panels. The yellow signals reflect the co-localization of GFP- or 6Myc-tagged Lats2 and the indicated proteins (Aurora-A or γ-tubulin). Scale bar, 10 μm.

of the S83-phosphorylated (pS83) Lats2 in HeLa S3 cells were analysed with the 3B11 antibody. As shown in Fig. 5(A), the phosphorylation signals of S83 by the 3B11 antibody were observed at the centrosomes of interphase and prometaphase cells (Fig. 5A,i and ii, left panels) and at the spindle poles of metaphase, anaphase and telophase cells (Fig. 5A,iii,iv and v, left panels). The centrosomal localization of pS83 was also confirmed by its co-localization with γ-tubulin (Fig. 5A,i–vi, right panels; yellow). The S83-phosphorylations of endogenous Lats2 and the subcellular localizations of GFP- and 6Myc-tagged Lats2 were observed at both a single centrosome and duplicated centrosomes during interphase (Figs 4 and 5, and data not shown). Centrosomes are duplicated during early S phase and mature during late S phase. Centrosomes then separate during early mitosis (reviewed in Doxsey 2001; Nigg 2002). Therefore, these results suggest that both the centrosomal localization and the initial S83-phosphorylations of Lats2 occur before S phase. The S83-phosphorylations at the centrosomes or the spindle poles were more prominent at prometaphase and metaphase (Fig. 5 and B,ii and iii, green spots) than at the other stages. These observations are similar to the subcellular localization of Aurora-A during the cell cycle (Fig. 5B). However, Aurora-A localizes to both the spindle poles and half-spindles, while the S83-phosphorylated Lats2 localizes only to the spindle poles during mitosis. Interestingly, during cytokinesis, while the S83-phosphorylation disappeared from the centrosomes or the spindle poles, it was detected at the midbody (Fig. 5A,vi and 5B-vi, left panels). It is noteworthy that this localization of pS83 during cytokinesis is more similar to that of Aurora-B than Aurora-A (Crosio *et al.* 2002). These results suggest that the endogenous Lats2 is localized to the centrosomes/the spindle poles, where it is phosphorylated on S83 by Aurora-A during the cell cycle.

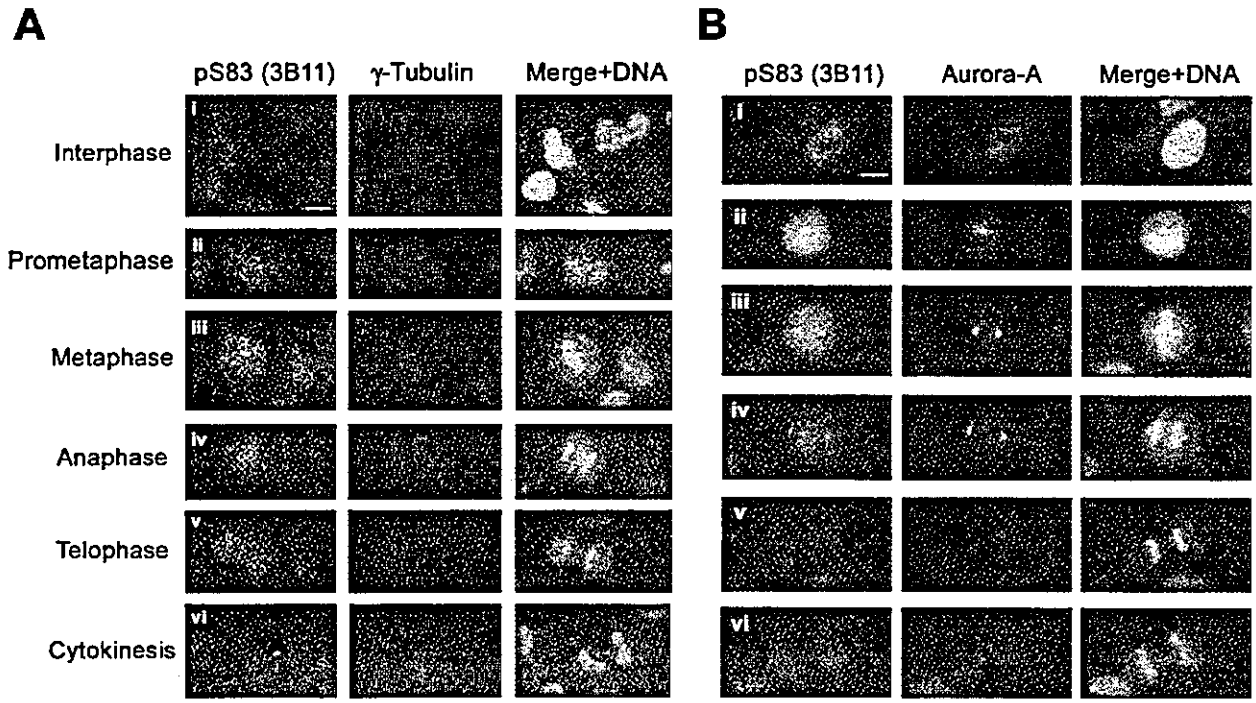

Figure 5 S83-phosphorylated Lats2 localizes to the centrosomes/spindle poles during the cell cycle besides cytokinesis. (A and B) HeLa S3 cells were synchronized at the S phase by thymidine-single block, released from the block and then fixed with formaldehyde at interphase (i), prometaphase (ii), metaphase (iii), anaphase (iv), telophase (v) and cytokinesis (vi). S83-phosphorylated Lats2 was visualized by immunofluorescence staining with the 3B11 antibody followed by incubation with Alexa-Fluor 488-conjugated anti-mouse immunoglobulin G (left panels, green). Centrosomes/spindle poles or Aurora-A were respective visualized with anti-γ-tubulin (A) or anti-Aurora-A (B) antibodies (2nd panels from left, red). DNA was visualized by staining with Hoechst 33258 (blue). DNA and merged images are shown in the right panels. The yellow signals indicate the co-localization of S83-phosphorylated Lats2 with the centrosomes/spindle poles. Scale bar, 10 μm.

Phosphorylation of S83 plays a role of the centrosomal localization of Lats2

To explore the significance of S83 phosphorylation in Lats2 localization, HeLa S3 cells were transfected with 6Myc-tagged full-length human Lats2 containing S83C or S83E (S83 mutated to glutamate), and the centrosomes were detected by staining with γ-tubulin (Fig. 6A and B, 2nd panels from left, red). The subcellular localization of both the S83C and S83E mutants during the cell cycle frequently showed mislocalization of Lats2 at the centrosome(s) of interphase HeLa S3 cells (Fig. 6A and B, top-left panel, arrows) in comparison with the 6Myc-Lats2 wild-type (Figs 4C and 6A and B; these experiments were performed in equal conditions). In mitotic cells, there is no detectable staining of the S83 mutant proteins (S83C, S83E) (Fig. 4A and B, bottom-left panels), as well as wild type (Fig. 4C). Therefore, we could not obtain any data on the centrosomal localization by comparison between each S83 mutant and wild type during all phases of mitosis. Next, among the cells expressing each 6Myc-Lats2 -WT, -S83C or -S83E, the numbers of cells in which the 6Myc-Lats2 obviously localized to the centrosome(s) during interphase were counted to assess the percentages of the centrosomal localization of Lats2 WT and two S83 mutants. As shown in Fig. 6(C), in 55% of cells expressing Lats2 WT, the 6Myc-Lats2 localized to the centrosome while, in the case of the S83C and S83E mutants, the percentage of cells harbouring the centrosomal Lats2 were reduced by less than 30 and 43%, respectively. These results indicate that the non-phosphorylation of the Ser 83 residue disturbs the centrosomal localization of Lats2.

Discussion

In this study, we have shown that Lats2 is phosphorylated in at least two distinct stages of the cell cycle, G_1/S phase and M phase containing nocodazole arrest (Fig. 1A and B), suggesting that Lats2 is regulated by multiple

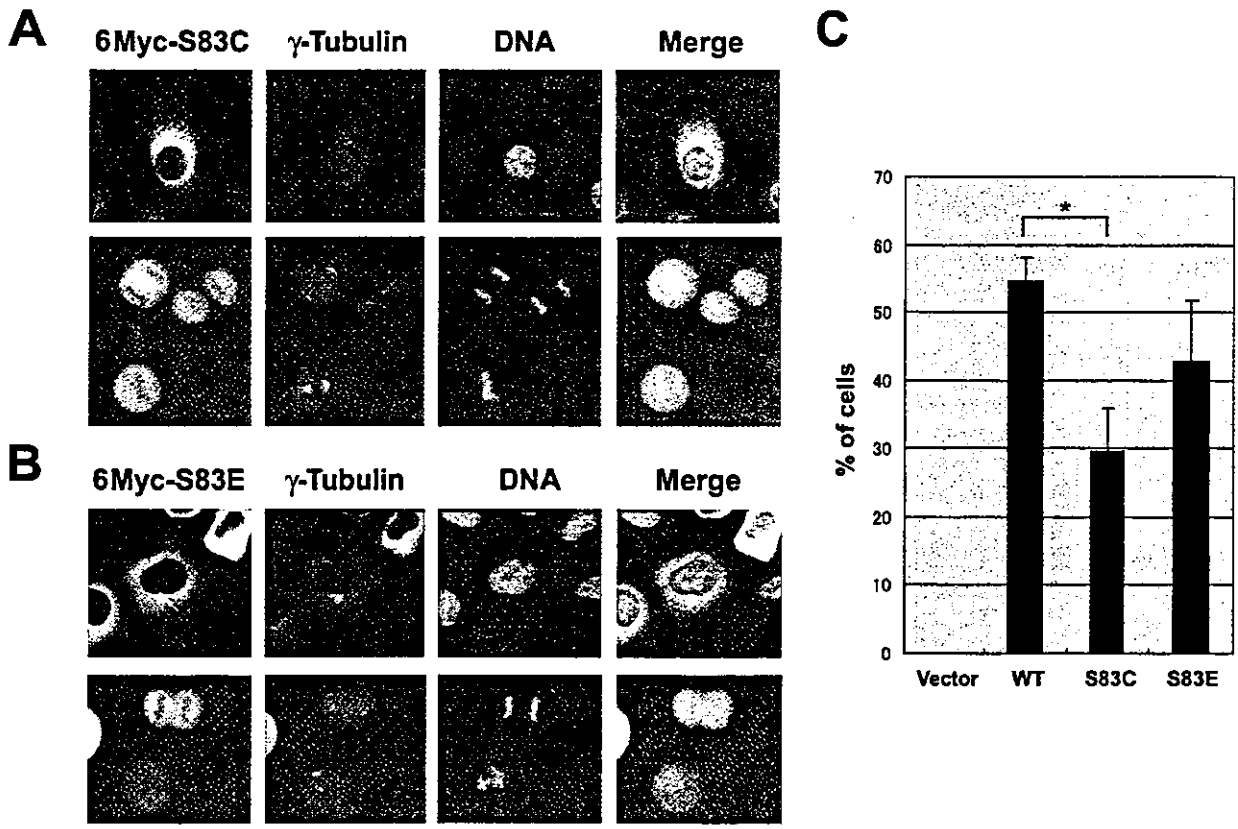

Figure 6 The phosphorylation of S83on Lats2 plays a role of its centrosomal localization. HeLa S3 cells were transiently transfected with 6Myc-tagged full-length Lats2-S83C (A) or 6Myc-tagged full-length Lats2-S83E (B). The transfected cells were fixed with formaldehyde at interphase (A-top and B-top panels), prometaphase (lower in B-bottom panel), metaphase (lower in A-bottom panel), anaphase (upper left in A-bottom panel) and telophase (upper right in A-bottom panel). 6Myc-Lats2 was visualized by immunofluorescence staining of the fixed cells with anti-Myc antibody followed by Alexa-Fluor 488-conjugated anti-mouse immunoglobulin G (A and B, green). Centrosomes were visualized by immunofluorescence staining with anti-γ-tubulin antibody (A and B, red), followed by Alexa Fluor 594-conjugated anti-rabbit immunoglobulin G. The positions of centrosomes are indicated by white arrows. DNA was visualized by staining with Hoechst 33258 (A and B, blue). Merged images are shown in the right panels. The yellow signals reflect the co-localization of the 6Myc-Lats2 proteins and γ-tubulin. (C) Histogram shows the percentages of cells in which the indicated 6Myc-tagged proteins localize to the interphase centrosomes in HeLa S3 cells. These results were obtained from four independent experiments (more than 50 positive cells in 500 cells each) and bars indicate standard deviations. All data were statistically analysed based on the Student's *t*-test. $*P = 0.001$.

phosphorylations throughout the cell cycle. Cyclin E/Cdk2 and Cyclin A/Cdk2 kinases alone could produce very weak phosphorylation signals on the degradation products of Lats2N (Fig. 1C). This observation might suggest that one of the phosphorylated forms of Lats2 during interphase may be due to Cyclin E/Cdk2 and Cyclin A/Cdk2 kinases. Because it is probable that mouse Lats2 also regulates the G_1/S transition through down-regulation of Cyclin E/Cdk2 kinase activity in NIH3T3 cells (Li *et al.* 2003), the G_1/S-dependent phosphorylation(s) of Lats2 that we have shown in Fig. 1(B) may be implicated in some functions of Lats2 on G_1/S transition. We identified a centrosomal kinase, Aurora-A, as one of the candidate kinases for phosphorylation of S83 residue on Lats2. Immunostaining data with the anti-phosphorylated S83 antibody reveals that S83 on Lats2 is phosphorylated *in vivo* during the cell cycle and it is more prominent during prophase and metaphase than interphase, anapahse and telophase, which is similar to the expression pattern of Aurora-A during the cell cycle (Fig. 4A and Bischoff *et al.* 1998). These results suggest that S83 on Lats2 is a phosphorylation target of Aurora-A *in vivo*. As Aurora-B and -C also phosphorylate Lats2, although very weakly (Fig. 2D), it will be important to examine in future whether Aurora-B or Aurora-C can more efficiently phosphorylate S83 or

other sites of Lats2 by using the full-length protein of Lats2. In fact, subcellular localization of phosphorylated S83 is observed at the midbody of cytokinesis cells, which is similar to that of Aurora-B (Fig. 5). Therefore, the phosphorylation of S83 on Lats2 may be regulated by not only Aurora-A but also Aurora-B.

Immunofluorescence data of exogenous GFP or 6Myc-tagged Lats2 protein indicate that Lats2 and Aurora-A co-localize at the centrosome during the cell cycle, except for metaphase and anaphase. We previously showed that Lats2 exists in the 'nuclear fraction' that was prepared from cell lysates by Western blot analysis (Yabuta *et al.* 2000). Probably, the centrosome was distributed in this fraction during our subfractionation procedure. Although a recent report of Li *et al.* has shown that ectopically expressed mouse Lats2 localized in the cytoplasm of NIH3T3 cells and that the majority of endogenous Lats2 protein is located in the cytoplasm in their fractionation experiments using lung cancer cells (Li *et al.* 2003). Moreover, the ectopic over-expression of Lats2 in cells tends to localize diffusely to the cytoplasm (Figs 4 and 6), which may be due to the degradation of exogenous Lats2 protein. However, our immunostaining data using the 3B11 antibody showed that endogenous Lats2 protein is located not only at centrosomes but also in the nucleus during interphase (Fig. 5A,i and B,i). These observations are consistent with the previous reports that Aurora-A localizes to both the centrosome and the nucleus during the G_2 phase (Crosio *et al.* 2002; Hirota *et al.* 2003). Recently, Aurora-A was reported to be required for mitotic entry of human cells in concert with its interacting activator Ajuba, a LIM protein. It is likely that Aurora-A is initially activated at the G_2 phase and its activity is required for the recruitment of the Cyclin B1/Cdc2 complex to centrosomes (Hirota *et al.* 2003). Although Lats2 localized to the centrosome before its duplication in early S phase, it is not possible that Lats2 is involved in the regulation of centrosomal duplication, because we could also observe two close spots of γ-tubulin, as well as typical and normal duplications of the centrosome, in HeLa cells in which the wild-type or the S83 mutants of Lats2 was over-expressed ectopically. Moreover, in accordance with a previous report on a role of *Drosophila* Aurora-A in centrosome maturation, Aurora-A promotes the recruitment of D-TACC to centrosomes and phosphorylates it (Giet *et al.* 2002). Because the phosphorylation of S83 on Lats2 is one of requirements for centrosomal localization of Lats2 in this issue, Aurora-A may also promote the recruitment of Lats2 to centrosomes as well as Cyclin B1/Cdc2 complex and D-TACC for the centrosome maturation. The accumulated Lats2 kinase at the centrosome may rapidly phosphorylate other centrosomal components, together with some centrosomal kinases including Cdc2 and Plk1, polo-like kinase, in order to progress the centrosome maturation efficiently. γ-Tubulin is one of the components that are recruited to the MTOC (microtubule-organizing centre) during the centrosome maturation. When the wild-type or the S83 mutants of Lats2 were over-expressed in HeLa cells, we could observe one or two spots of γ-tubulin in these cells (Figs 4 and 6), which is suggestive of the recruitment of γ-tubulin to MTOC. Therefore, it is unlikely that Lats2 is involved, at least in the recruitment of γ-tubulin. Moreover, the over-expression of the wild-type or the S83 mutants of Lats2 did not cause abnormal chromosome alignment and aberrant mitotic spindle formation (Figs 4 and 6, and data not shown). To date, several structurally different protein kinases, including Aurora kinases and Cdks, have been shown to localize at the centrosome regulating the centrosomal function during the cell cycle (Mayor *et al.* 1999). Among these proteins, Nek2, as a NIMA-like kinase and Plk1 are representative centrosomal kinases, although Nek2 could not phosphorylate Lats2 *in vitro*. Although as yet untested, it is intriguing whether Plk1 also phosphorylates Lats2 because Plk1 is involved in not only controlling centrosomal functions but also DNA damage checkpoint (Smits *et al.* 2000). However, the GFP-Lats2 or 6Myc-Lats2-specific signal was diffusely distributed throughout the cell but not at the centrosome during mitosis (Fig. 4). By using the 3B11 antibody, we could observe that endogenous Lats2 localizes at the centrosome or the spindle pole during mitosis. Therefore, the diffusely distribution of GFP- and 6Myc-Lats2 may also be due to the effects of over-expression of these proteins in a mitotic cell, including the protein degradation.

When the kinase activities of these Lats2 mutants were assessed by examining the auto-phosphorylation of immunoprecipitates generated by the anti-GFP antibody from extracts expressing GFP-Lats2 wild-type or S83C mutant, we were unable to observe remarkable differences in their phosphorylation levels (data not shown). A previous report has shown that over-expression of either wild-type or kinase inactive form of Aurora-A in HeLa cells triggered mitotic defects including aberrant cytokinesis and the formation of tetraploid cells, but not centrosome amplification in S phase (Meraldi *et al.* 2002). Therefore, we suppose that the Aurora-A-dependent phosphorylation of S83 on Lats2 is not implicated in the aberrant cytokinesis and the formation of tetraploid cells caused by over-expression of Aurora-A in HeLa cells. On this issue, we showed that S83 phosphorylation plays a role of the centrosomal localization of Lats2 (Fig. 6). It

is noteworthy that there is no detectable staining of the S83 mutant proteins in telophase cells, although this is seen in cells expressing the wild-type protein (Fig. 6A and B). Therefore, it can be speculated that the phosphorylation of S83 may be involved in not only its centrosomal localization but also its midbody localization during cytokinesis. Moreover, we showed that all of the cells expressing S83C mutant are not localized to the centrosome (Fig. 6C). The result suggests that the phosphorylation of S83 is not the only cause for centrosomal localization of Lats2 and therefore further studies are required. Recently, a report has shown that Lats2 kinase activity and two LATS conserved domains (LCD1 and LCD2), two stretches of highly conserved sequence in amino-terminus between Lats1 and Lats2, are required for Lats2 to suppress tumorigenicity and to inhibit cell proliferation (Li *et al.* 2003). It is notable that S83 locates in LCD1. The phosphorylation of S83 by Aurora-A may be important for Lats2 to suppress tumorigenicity and to inhibit cell proliferation via centrosomal regulations.

Taken together, our data suggest that Lats2 is a novel centrosome-associated kinase that may be involved in regulating the centrosome and/or mitotic spindle downstream of Aurora-A.

Experimental procedures

Cell culture, cell cycle synchronization and transfections

All cell lines were maintained in Dulbecco's modified Eagle's medium (DMEM) with 10% foetal calf serum (FCS, HyClone, Logan, UT, USA), 100 U/mL penicillin and 100 μg/mL streptomycin. HeLa cells were synchronized to enter the G_1/S phase by the thymidine-aphidicoline double block and release protocol (Tsuruga *et al.* 1997). Cells at the G_2/M phase were collected 9 h after release. Mitotic cells were only obtained by shaking-off after incubation for 18 h in medium containing 80 ng/mL nocodazole. Cell synchrony was monitored by Western blotting with anti-Cyclin B antibody or by FACS analysis (Becton-Dickinson, Franklin Lakes, NJ, USA). Transient transfection of HeLa S3 and 293T cells were carried out using LipofectAMINE or PLUS reagents according to the manufacturer's instructions (Invitrogen, Carlsbad, CA, USA).

Plasmids and site-directed mutagenesis

To isolate the complete human *LATS2* cDNA, we screened a human placenta cDNA library (Clontech), using as a probe *Hin*dIII-*Pst*I fragments from the pAP3neo-*HsLATS2* plasmid that contains partial Lats2 cDNA (Yabuta *et al.* 2000). The nucleotide sequences of both strands of the isolated clone were determined by the dideoxy chain termination method. To construct the pCMVmyc-Lats2 full plasmid, we prepared *Bam*HI-*Xcm*I fragments by polymerase chain reaction (PCR) using the isolated clone as a template. These fragments were inserted into the *Bam*HI and *Xcm*I sites of the pCMV-*HsLATS2* plasmid (Yabuta *et al.* 2000). For expression in bacteria, full Lats2 cDNA was released from the pCMVmyc-Lats2 full plasmid by *Bam*HI and *Xho*I cleavage and recloned into the pGEX4T vector to produce pGEX4T-Lats2 (Amersham Pharmacia Biotech, Piscataway, NJ, USA). pGEX-Lats2N was constructed by ligating the *Eco*RI-*Hpa*I fragment from pAP3neo-*HsLATS2* into *Eco*RI and *Sma*I sites of pGEX4T2. pGEX-Lats2C was constructed by ligating the *Bam*HI-*Xho*I fragment from another plasmid, pCMVmyc-Lats2C, into the *Bam*HI and *Xho*I sites of pGEX4T. The pCMVmyc-Lats2C plasmid had been constructed by ligating the *Hinc*II-*Not*I fragment from pAP3neo-*HsLATS2* into the *Eco*RV and *Not*I sites of pCMVmyc. pGEX-Lats2-79-257 was constructed by digesting pGEX-Lats2N with *Not*I followed by self-ligation. pCMV6myc-Lats2 full was constructed by ligating the *Bam*HI-*Xho*I fragment from pCMVmyc-Lats2 full into the *Bam*HI and *Xho*I sites of pCMV6myc. pCMV6myc-Lats2-1-393 was constructed by ligating the *Bam*HI-*Pml*I fragment from pGEX-Lats2 into the *Bam*HI and *Eco*RV sites of pCMV6myc. The other truncated Lats2 mutants were constructed in pGEX4T by PCR with the following primers which contain either an *Eco*RI site or a *Xho*I site: Lats2-1-78, F11 (5′-CCGGAATTCATGAGGCCAAAGAGTTTTCCT-3′) and R9 (5′-ATACTCGAGCCTCAAGGCTTTCTGATAAGG-3′); 1-118, F11 and R3 (5′-ATACTCGAGGCCAGCCATCTCCTGGTC-3′); 79-118, F2 (5′-GCGGAATTCGAAATCAGATAT TCCTTGTTG-3′) and R3; 79-151, F2 and R2 (5′-ATACTCGAGCGCACAATCTGCTCATTCC-3′); 113-151, F3 (5′-ATAGAATTCGACCAGGAGATGGCTGGC-3′) and R2. All point mutants of Lats2 and Aurora-A KD (kinase dead: D273E) (Shindo *et al.* 1998) were generated by site-directed mutagenesis using the QuickChange Site-Directed Mutagenesis Kit (Stratagene, La Jolla, CA, USA) according to the manufacturer's instructions. Aurora-A (Aik2) (Zhou *et al.* 1998), Aurora-B (AIM1) (Tatsuka *et al.* 1998) and Aurora-C (AIE2) (Tseng *et al.* 1998) cDNA were generated by PCR from the human placenta cDNA library. All amplified sequences were confirmed by DNA sequencing.

Expression and purification of recombinant proteins

For the expression of GST-fused Lats2 mutants, Aurora-A, Aurora-B, Aurora-C and Aurora-A KD, pGEX plasmids with the appropriate cDNAs were introduced into bacteria. The cultures were induced with 0.5 mM isopropyl β-D-thiogalactopyranoside (IPTG) and incubated at 37 °C for 6 h. Cells were collected and lysed in PBS containing 1% Triton X-100, 2 μg/mL leupeptin, 10 μg/mL aprotinin, 1 mM PMSF, 1 mM benzamidine, 1 mM NaF and 1 mM Na_3VO_4 by brief sonication. After centrifugation, the clear lysate was adsorbed to Glutathione Sepharose 4B (Amersham Pharmacia Biotech) and eluted with 10 mM reduced glutathione. GST-DNA-PK, GST-Nek2, GST-Nop10 and active Cyclin-Cdk kinase complexes (Cyclin D1/Cdk4, Cyclin B/Cdc2, Cyclin E/Cdk2 and Cyclin A/Cdk2) were obtained from MBL Co. Ltd (Japan). Rb C-terminus (amino acids 701-928) was purchased from New England Biolabs (Beverly, MA, USA).

Antibodies

The generation and specificity of the 3D10 anti-human Lats2 monoclonal antibody has been previously described (Yabuta *et al.* 2000). To generate an anti-Aurora-A polyclonal antibody, rabbits were injected with a recombinant GST-fused full-length Aurora-A protein. The antisera were then affinity-purified against the protein. Anti-γ-tubulin polyclonal antibody (Sigma, St Louis, MO, USA) was purchased. Anti-HA polyclonal, anti-Cyclin B, anti-Myc and anti-GST monoclonal antibodies were obtained from MBL Co. Ltd.

Generation of anti-phospho-Ser83 monoclonal antibody and Western blotting

To establish a mouse hybridoma that produces anti-phospho-S83-Lats2 antibodies, mice were immunized subcutaneously with the KLH-conjugated phosphopeptide CREIRYS(PO_3H_2)LLPF (amino acids 78–87) emulsified in Freund's complete adjuvant. Thereafter, the mice were boosted four times at biweekly intervals with the KLH conjugate in Freund's incomplete adjuvant. B-cell hybridomas were generated from the spleen cells of these mice and the 3B11 anti-phospho-S83 antibody was affinity-purified by the phospho-antigen-peptide column. To eliminate non-specific antibodies reacting with the unphosphorylated antigen peptide, the antibody preparation was passed through a non-phospho-Lats2-peptide (CREIRYSLLPF) column. The specificity of the 3B11 antibody was confirmed by both Western blotting (shown in Fig. 3C) and ELISA (data not shown). To detect the *in vivo* phosphorylation of S83, immunoprecipitations were performed with 5 μg of either the 3D10 or 3B11 antibody, after which the immunoprecipitates were resolved by SDS–PAGE and transferred to polyvinylidene difluoride (PVDF) membranes (Millipore Corporation, Bedford, MA, USA). Western blotting was performed with 5 μg of 3D10 antibody in TBST (100 mM Tris-Cl, pH 7.5, 150 mM NaCl, 0.05% Tween-20) containing 1% BSA. Western blotting using antibodies other than 3D10 and 3B11 was performed in TBST containing 5% non-fat milk.

In vitro kinase assays and immunoprecipitations

In vitro kinase assays were performed with 1 μg of GST-purified kinases and 2 μg of GST-purified substrates for 30 min at 30 °C in kinase buffer (20 mM Tris-HCl, pH 7.5, 10 mM $MgCl_2$, 5 mM $MnCl_2$, 1 mM DTT, 1 mM NaF, 0.1 mM Na_3VO_4, 10 mM β-glycerophosphate) containing 20 μM ATP and 10 μCi [γ-^{32}P]ATP. To examine the interaction between 6Myc-Lats2 and 1-393 and GFP-Aurora-A, the transfected 293T cells were lysed in lysis buffer A (50 mM Tris-HCl, pH 7.5, 250 mM NaCl, 1 mM EDTA, 0.2% NP-40, 1 mM PMSF, 1 μg/mL aprotinin, 2 μg/mL leupeptin, 1 μg/mL pepstatine A, 1 mM NaF, 1 mM Na_3VO_4). After centrifugation, the clear lysates were immunoprecipitated with 2 μg of anti-Myc or anti-GFP antibodies for 3 h at 4 °C. The immune complexes were collected by adding 30 μL of 50% protein G sepharose (Amersham Pharmacia Biotech) slurry. The complexes were washed five times with lysis buffer B (50 mM Tris-HCl, pH 7.5, 50 mM NaCl, 1 mM EDTA, 0.1% NP-40).

Immunofluorescence staining

HeLa S3 cells that transiently expressed GFP-full length Lats2 or GFP alone were fixed by sequential incubations with 4% formaldehyde in PBS, 0.1% Triton X-100 in PBS and then 0.05% Tween-20 in PBS, each for 10 min at room temperature. To prepare mitotic cells, the transfected cells were blocked at the S phase by the addition of 2.5 mM thymidine for 22 h. They were then released from the block by replacing the medium with fresh medium without drugs. They were fixed 12 h later. After being washed, cells were incubated with anti-Aurora-A antibody or anti-γ-tubulin antibody, followed by incubation with Texas Red (Amersham Pharmacia Biotech) or AlexaFluor 594 (Molecular Probes, Eugene, OR, USA)-conjugated anti-rabbit/mouse immunoglobulin G as previously described (Tsuruga *et al.* 1997). To visualize 6Myc-Lats2 or its derivatives, cells expressing each 6Myc-Lats2 derivative were fixed and stained with anti-Myc antibody followed by Alexa-Fluor 488-conjugated anti-mouse immunoglobulin G. DNA was stained by Hoechst 33258 (Sigma). Immunofluorescence staining with the 3B11 antibody was performed as similar way. The stained cells were observed with an Axiophot microscope (Zeiss) or BX51 microscope (Olympus).

Acknowledgements

We thank Dr P. Hughes for critically reading the manuscript. This work was supported by a Grant-in-aid for Scientific Research on Priority Areas from the Ministry of Education, Culture, Sports, Science and Technology of Japan, and grants from the Osaka Cancer Society, the Yasuda Medical Research Foundation, the Welfide Medical Research Foundation, the Japanese Foundation for Multidisciplinary Treatment of Cancer and the Osaka Cancer Research Foundation.

References

Adams, R.R., Carmena, M. & Earnshaw, W.C. (2001) Chromosomal passengers and the (aurora) ABCs of mitosis. *Trends Cell Biol.* **11**, 49–54.

Anand, S., Penrthyn-Lowe, S. & Venkitaraman, A.R. (2003) AURORA-A amplification overrides the mitotic spindle assembly checkpoint, inducing resistance to Taxol. *Cancer Cell* **3**, 51–62.

Bischoff, J.R. & Plowman, G.D. (1999) The Aurora/Ipl1p kinase family: regulators of chromosome segregation and cytokinesis. *Trends Cell Biol.* **9**, 454–459.

Bischoff, J.R., Anderson, L., Zhu, Y., *et al.* (1998) A homologue of *Drosophila aurora* kinase is oncogenic and amplified in human colorectal cancers. The Aurora/Ipl1p kinase family: regulators of chromosome segregation and cytokinesis. *EMBO J.* **17**, 3052–3065.

Blagden, S.P. & Glover, D.M. (2003) Polar expeditions-provisioning the centrosome for mitosis. *Nature Cell Biol.* **5**, 505–511.

Chen, S.-S., Chang, P.-C., Cheng, Y.-W., Tang, F.-M. & Lin, Y.-S. (2002) Suppression of the STK15 oncogenic activity requires a transactivation-independent p53 function. *EMBO J.* **21**, 4491–4499.

Crosio, C., Fimia, M.F., Loury, R., *et al.* (2002) Mitotic phosphorylation of histone H3: spatio-temporal regulation by mammalian Aurora kinases. *Mol. Cell. Biol.* **22**, 874–885.

Doxsey, S. (2001) Re-evaluating centrosome function. *Nature Rev. Mol. Cell Biol.* **2**, 688–698.

Dutertre, S., Descamps, S. & Prigent, C. (2002) On the role of aurora-A in centrosome function. *Oncogene* **21**, 6175–6183.

Eyers, P.A., Erikson, E., Chen, L.G. & Maller, J.L. (2003) A novel mechanism for activation of the protein kinase Aurora A. *Curr. Biol.* **13**, 691–697.

Farruggio, D.C., Townsley, F.M. & Ruderman, J.V. (1999) Cdc20 associates with the kinase aurora2/Aik. *Proc. Natl. Acad. Sci. USA* **96**, 7306–7311.

Fry, A.M., Schultz, S.J., Bartek, J. & Nigg, E.A. (1995) Substrate specificity and cell cycle regulation of the Nek2 protein kinase, a potential human homolog of the mitotic regulator NIMA of *Aspergillus nidulans*. *J. Biol. Chem.* **270**, 12899–12905.

Giet, R. & Prigent, C. (1999) Aurora/Ipl1p-related kinases, a new oncogenic family of mitotic serine-threonine kinases. *J. Cell Sci.* **112**, 3591–3601.

Giet, R., McLean, D., Descamps, S., *et al.* (2002) *Drosophila* Aurora A kinase is required to localize D-TACC to centrosomes and to regulate astral microtubules. *J. Cell Biol.* **156**, 437–451.

Glover, D.M., Leibowitz, M.H., McLean, D.A. & Parry, H. (1995) Mutations in aurora prevent centrosome separation leading to the formation of monopolar spindles. *Cell* **81**, 95–105.

Henras, A., Henry, Y., Bousquet-Antonelli, C., *et al.* (1998) Nhp2p and Nop10p are essential for the function of H/ACA snoRNPs. *EMBO J.* **17**, 7078–7090.

Hirota, T., Morisaki, T., Nishiyama, Y., *et al.* (2000) Zyxin, a regulator of actin filament assembly, targets the mitotic apparatus by interacting with h-warts/LATS1 tumor suppressor. *J. Cell Biol.* **149**, 1073–1086.

Hirota, T., Kunitoku, N., Sasayama, T., *et al.* (2003) Aurora-A and an interacting activator, the LIM protein Ajuba, are required for mitotic commitment in human cells. *Cell* **114**, 585–598.

Hori, T., Takahori-Kondo, A., Kamikubo, Y. & Uchiyama, T. (2000) Molecular cloning of a novel human protein kinase, kpm, that is homologous to warts/lats, a *Drosophila* tumor suppressor. *Oncogene* **19**, 3101–3109.

Justice, R.W., Zelian, O., Woods, D.F., Noll, M. & Bryant, P.J. (1995) The *Drosophila* tumor suppressor gene *warts* encodes a homolog of human myotonic dystrophy kinase and is required for the control of cell shape and proliferation. *Genes Dev.* **9**, 534–546.

Kamikubo, Y., Takaori-Kondo, A., Uchiyama, T. & Hori, T. (2003) Inhibition of cell growth by conditional expression of kpm, a human homologue of *Drosophila* warts/lats tumor suppressor. *J. Biol. Chem.* **278**, 17609–17614.

Katayama, H., Zhou, H., Li, Q., Tatsuka, M. & Sen, S. (2001) Interaction and feedback regulation between STK15/BTAK/Aurora-A kinase and protein phosphatase 1 through mitotic cell division cycle. *J. Biol. Chem.* **276**, 46219–46224.

Kim, S.-T., Lim, D.-S., Canman, C.E. & Kastan, M. (1999) Substrate specificities and identification of putative substrates of ATM kinase family members. *J. Biol. Chem.* **274**, 37538–37543.

Kimura, M., Matsuda, Y., Yoshioka, T. & Okano, Y. (1999) Cell cycle-dependent expression and centrosome localization of a third human aurora/Ipl1-related protein kinase, AIK3. *J. Biol. Chem.* **274**, 7334–7340.

Kitagawa, M., Higashi, H., Jung, H.K., *et al.* (1996) The consensus motif for phosphorylation by cyclin D1-Cdk4 is different from that for phosphorylation by cyclin A/E-Cdk2. *EMBO J.* **15**, 7060–7069.

Kufer, T.A., Sillje, H.H., Korner, R., *et al.* (2002) Human TPX2 is required for targeting Aurora-A kinase to the spindle. *J. Cell Biol.* **158**, 617–623.

Li, Y., Pei, J., Xia, H., *et al.* (2003) Lats2, a putative tumor suppressor, inhibits G1/S transition. *Oncogene* **22**, 4398–4405.

Mayor, T., Meraldi, P., Stierhof, Y.D., Nigg, E.A. & Fry, A.M. (1999) Protein kinases in control of the centrosome cycle. *FEBS Lett.* **452**, 92–95.

Meraldi, P., Honda, R. & Nigg, E.A. (2002) Aurora-A overexpression reveals tetraploidization as a major route to centrosome amplification in p53-/- cells. *EMBO J.* **21**, 483–492.

Morisaki, T., Hirota, T., Iida, S., *et al.* (2002) WARTS tumor suppressor is phosphorylated by Cdc2/cyclin B at spindle poles during mitosis. *FEBS Lett.* **529**, 319–324.

Nigg, E.A. (2001) Mitotic kinases as regulators of cell division and its checkpoints. *Nature Rev. Mol. Cell Biol.* **2**, 21–32.

Nigg, E.A. (2002) Centrosome aberrations: cause or consequence of cancer progression? *Nature Rev. Cancer* **2**, 815–825.

Nishiyama, Y., Hirota, T., Morisaki, T., *et al.* (1999) A human homolog of *Drosophila warts* tumor suppressor, h-warts, localized to mitotic apparatus and specifically phosphorylated during mitosis. *FEBS Lett.* **459**, 159–165.

Shindo, M., Nakano, H., Kuroyanagi, H., *et al.* (1998) cDNA cloning, expression, subcellular localization, and chromosomal assignment of mammalian aurora homologues, aurora-related kinase (ARK) 1 and 2. *Biochem. Biophys. Res. Commun.* **244**, 285–292.

Smits, V.A., Klompmaker, R., Arnaud, L., *et al.* (2000) Polo-like kinase-1 is a target of the DNA damage checkpoint. *Nature Cell Biol.* **2**, 672–676.

St. John, M.A.R., Tao, W., Fei, X., *et al.* (1999) Mice deficient of *Lats1* develop soft-tissue sarcomas, ovarian tumours and pituitary dysfunction. *Nature Genet.* **21**, 182–186.

Tao, W., Zhang, S., Turenchalk, G.S., *et al.* (1999) Human homologue of the *Drosophila melanogaster lats* tumour suppressor modulates CDC2 activity. *Nature Genet.* **21**, 177–181.

Tatsuka, M., Katayama, H., Ota, T., *et al.* (1998) Multinuclearity and increased ploidy caused by overexpression of the aurora- and Ipl1-like midbody-associated protein mitotic kinase in human cancer cells. *Cancer Res.* **58**, 4811–4816.

Tsai, M.Y., Wiese, C., Cao, K., *et al.* (2003) A Ran signalling pathway mediated by the mitotic kinase Aurora A in spindle assembly. *Nature Cell Biol.* **5**, 242–248.

Tseng, T.C., Chen, S.H., Hsu, Y.P. & Tang, T.K. (1998) Protein kinase profile of sperm and eggs: cloning and characterization of two novel testis-specific protein kinases (AIE1, AIE2) related to yeast and fly chromosome segregation regulators. *DNA Cell Biol.* **17**, 823–833.

Tsuruga, H., Yabuta, N., Hosoya, S., *et al.* (1997) *HsMCM6*: a new member of the human MCM/P1 family encodes a protein homologous to fission yeast Mis5. *Genes Cells* **2**, 381–399.

Xia, H., Qi, H., Li, Y., *et al.* (2002) LATS1 tumor suppressor regulates G2/M transition and apoptosis. *Oncogene* **21**, 1233–1241.

Xu, T., Wang, W., Zhang, S., Stewart, R.A. & Yu, W. (1995) Identifying tumor suppressors in genetic mosaics: the *Drosophila lats* gene encodes a putative protein kinase. *Development* **121**, 1053–1063.

Yabuta, N., Fujii, T., Copeland, N.G., *et al.* (2000) Structure, expression, and chromosome mapping of *LATS2*, a mammalian homologue of the *Drosophila* tumor suppressor gene *lats/warts*. *Genomics* **63**, 263–270.

Yang, X., Li, D.M., Chen, W. & Xu, T. (2001) Human homologue of *Drosophila lats*, LATS1, negatively regulate growth by inducing G(2)/M arrest or apoptosis. *Oncogene* **20**, 6516–6523.

Zhou, H., Kuang, J., Zhong, L., *et al.* (1998) Tumour amplified kinase STK15/BTAK induces centrosome amplification, aneuploidy and transformation. *Nature Genet.* **20**, 189–193.

Received: 14 October 2003
Accepted: 2 February 2004

Mcp6, a meiosis-specific coiled-coil protein of *Schizosaccharomyces pombe*, localizes to the spindle pole body and is required for horsetail movement and recombination

Takamune T. Saito, Takahiro Tougan, Daisuke Okuzaki, Takashi Kasama and Hiroshi Nojima*

Department of Molecular Genetics, Research Institute for Microbial Diseases, Osaka University, 3-1 Yamadaoka, Suita, Osaka 565-0871, Japan

*Author for correspondence (e-mail: snj-0212@biken.osaka-u.ac.jp)

Accepted 3 November 2004
Journal of Cell Science 118, 447-459 Published by The Company of Biologists 2005
doi:10.1242/jcs.01629

Summary

We report here that a meiosis-specific gene of *Schizosaccharomyces pombe* denoted *mcp6*$^+$ (meiotic coiled-coil protein) encodes a protein that is required for the horsetail movement of chromosomes at meiosis I. The *mcp6*$^+$ gene is specifically transcribed during the horsetail phase. Green fluorescent protein (GFP)-tagged Mcp6 appears at the start of karyogamy, localizes to the spindle-pole body (SPB) and then disappears before chromosome segregation at meiosis I. In the *mcp6Δ* strain, the horsetail movement was either hampered (zygotic meiosis) or abolished (azygotic meiosis) and the pairing of homologous chromosomes was impaired. Accordingly, the allelic recombination rates of the *mcp6Δ* strain were only 10-40% of the wild-type rates. By contrast, the ectopic recombination rate of the *mcp6Δ* strain was twice the wild-type rate. This is probably caused by abnormal homologous pairing in *mcp6Δ* cells because of aberrant horsetail movement. Fluorescent microscopy indicates that SPB components such as Sad1, Kms1 and Spo15 localize normally in *mcp6Δ* cells. Because Taz1 and Swi6 also localized with Sad1 in *mcp6Δ* cells, Mcp6 is not required for telomere clustering. In a *taz1Δ* strain, which does not display telomere clustering, and the *dhc1-d3* mutant, which lacks horsetail movement, Mcp6 localized with Sad1 normally. However, we observed abnormal astral microtubule organization in *mcp6Δ* cells. From these results, we conclude that Mcp6 is necessary for neither SPB organization nor telomere clustering, but is required for proper astral microtubule positioning to maintain horsetail movement.

Supplementary material available online at
http://jcs.biologists.org/cgi/content/full/118/2/447/DC1

Key words: Meiosis, *S. pombe*, SPB, Recombination, Pairing, Horsetail

Introduction

Sexually reproducing eukaryotic organisms undergo meiosis, a special type of cell division, to generate inheritable haploid gametes from diploid parental cells. This process includes meiosis-specific events that increase genetic diversity, such as synaptonemal complex (SC) formation, homologous pairing and recombination. The fission yeast *Schizosaccharomyces pombe* proceeds to meiosis when it is nutritionally starved. At this point, two cells with opposite mating types conjugate and the two haploid nuclei fuse, thereby producing a zygote with a diploid nucleus; the meiotic process immediately follows this. Efficient pairing of the homologous chromosomes and the subsequent processing and completion of recombination during the meiotic prophase are pivotal for achieving correct chromosome segregation during meiotic division. An essential event for efficient chromosome pairing in *S. pombe* is the clustering during prophase of meiosis I of the telomeres of three chromosomes near the spindle-pole body (SPB) (Chikashige et al., 1994; Chikashige et al., 1997). This characteristic arrangement of meiotic chromosomes has been observed in a wide range of organisms and is denoted a 'bouquet' arrangement (Loidl, 1990; Scherthan, 2001; Zickler and Kleckner, 1999). This arrangement has been proposed to facilitate homologous chromosome pairing because it generates a polarized chromosome configuration by bundling chromosomes together at their telomeres.

The clustering of telomeres occurs during an event termed horsetail nuclear movement that is characteristic of *S. pombe*. It occurs at prophase I of meiosis and is characterized by a dynamic oscillation of the nucleus and the adoption by the nucleus of an elongated morphology (Chikashige et al., 1994). This movement has been proposed to facilitate the pairing of homologous chromosomes because it causes the chromosomes, which are aligned in the same direction as a result of bundling at their telomeric ends, to be shuffled around each other (Chikashige et al., 1994; Kohli, 1994; Hiraoka, 1998; Yamamoto et al., 1999; Yamamoto and Hiraoka, 2001). Thus, it enhances the chance that a chromosome encounters its correct partner and thereby promotes the linkage of homologous pairs of chromosomes through homologous recombination. In support of this notion, homologous recombination is reduced in mutants that display impaired

telomere clustering owing to the depletion of protein components of the telomere or the SPB, even though recombination machinery is intact in these mutants. For example, elimination of the telomere-binding protein Taz1 (Cooper et al., 1998; Nimmo et al., 1998) or Rap1 (Kanoh and Ishikaw, 2001), or depletion of the SPB component Kms1 (Shimanuki et al., 1997; Niwa et al., 2000) results in a loss of telomere-SPB clustering and reduced meiotic recombination.

It has been proposed that horsetail nuclear movement is predominantly established by pulling the astral microtubules that link the SPB to microtubule-anchoring sites, and that the pulling force is provided by cytoplasmic dynein (Chikashige et al., 1994; Svoboda et al., 1995; Ding et al., 1998; Yamamoto and Hiraoka, 2003). Thus, homologous recombination is also reduced when nuclear oscillation is abolished by disrupting the *dhc1*$^+$ gene, which encodes dynein heavy chain (DHC), a major component of cytoplasmic dynein that is localized to microtubules and the SPB (Yamamoto et al., 1999). It was proposed that dynein drives this nuclear oscillation by mediating the cortical microtubule interactions and regulating the dynamics of microtubule disassembly at the cortex (Yamamoto et al., 2001). Meiotic recombination is also reduced in a null mutant of the *dlc1*$^+$ gene that encodes an SPB protein that belongs to the dynein-light-chain family (Miki et al., 2003). In this mutant, Dhc1-dependent nuclear movement during meiotic prophase is irregular in its duration and direction. This model explains some of the regulatory mechanisms behind nuclear oscillation and chromosome pairing. However, the details of these mechanisms are still mostly unknown. The identification of additional regulatory components is needed fully to elucidate these processes.

In the course of our functional characterization of meiotic-specific proteins that harbour coiled-coil motifs, we found a new SPB-associated protein that is required for meiotic nuclear oscillation and recombination. This gene is expressed specifically during meiosis and thus is referred to as *mcp6*$^+$ (meiotic coiled-coil protein). The coiled-coil motif, which consists of two to five amphipathic α-helices that twist around one another to form a supercoil, is known to be required for protein-protein interaction (Burkhard et al., 2001). In the present study, we report our functional analysis of this protein.

Materials and Methods

Yeast strains, media and molecular biology

The *S. pombe* strains used in this study are listed in Table 1. Complete media YPD or YE, the synthetic minimal medium EMM2 and the sporulation media ME or EMM2-N (1% glucose) were used (Alfa et al., 1993). Homozygous diploid strains were constructed by cell fusion. Cells were converted to protoplasts by treatment with lysing enzyme. Then, cells were fused using $CaCl_2$ and polyethylene glycol (Sipiczki and Ferenczy, 1977). Plates with EMM2 containing 1 M sorbitol were used in the cell fusion experiments. Induction of meiosis in the genetic background of the *pat1-114* mutant (Shimada et al., 2002). Northern (Watanabe et al., 2001) and western blot (Okuzaki et al., 2003) analyses were performed as described previously.

Gene disruption

To disrupt the *mcp6*$^+$ gene by replacing it with the *ura4*$^+$ gene, we used the polymerase chain reaction (PCR) to obtain a DNA fragment carrying the 5′ upstream region and 3′ downstream region of the *mcp6*$^+$ gene. For this purpose, we synthesized the following four oligonucleotides and used them as primers: mcp6-5F, 5′-GGTAC-CTTCTGGTGCCGCCGACCTTC-3′; mcp6-5R, 5′-CTCGAGAT-TAAATCAATCTGTTAATC-3′; mcp6-3F, 5′-CCCGGGGGATAGC-TATGAAACCCTGA-3′; mcp6-3R, 5′-GAGCTCTCATTTTTTT-TATAAGAAGG-3′. (The underlined sequences denote the artificially introduced restriction enzyme sites for *Kpn*I, *Xho*I, *Sma*I and *Sac*I, respectively.) These PCR products and the 1.8 kb *Hin*dIII fragment containing the *ura4*$^+$ gene (Grimm et al., 1988) were inserted into the pBluescriptII KS (+) vector via the *Kpn*I-*Xho*I, *Sma*I-*Sac*I or *Hin*dIII sites. This plasmid construct was digested with *Kpn*I and *Sac*I, and the resulting construct was introduced into the diploid strain TP4-5A/TP4-1D. The Ura$^+$ transformants were then screened by Southern blot analysis to identify the disrupted strain.

Construction of strains harbouring integrated *mcp6*$^+$-tag genes

To construct green fluorescent protein (GFP)-tagged *mcp6*$^+$ strains, we performed PCR using the wild-type (TP4-5A) genome as a template and obtained a DNA fragment carrying the open reading frame (ORF) region and the 3′ downstream region of the *mcp6*$^+$ gene. For this purpose, we synthesized the following two oligonucleotides and used them as primers: mcp6-ORF-F, 5′-CGGCGCGCCG-CATATGGAATATCAAGAAGAGGC-3′; mcp6-ORF-R, 5′-GTA-CTCGAGGCGGCCGCGGGCTCAGATCGTGATTGACAG3′. The underlined sequences denote the artificially introduced restriction enzyme sites for *Asc*I and *Nde*I, and *Xho*I and *Not*I, respectively. To obtain the 3′ downstream region, we used the same primers as described above. These PCR products were inserted into the pTT(GFP)-Lys3 vector (T.T., unpublished) (see supplementary material Fig. S1), which is designed to allow one-step integration via *Nde*I-*Not*I and *Sma*I-*Sac*I sites. This plasmid construct was digested with *Pme*I. The resulting construct was introduced into strain HM105 (*h*$^-$ *lys3*). We then screened the Lys$^+$ transformants and confirmed the precise integration of the constructs by PCR.

Recombination frequency and spore viability

The crossing-over rate was determined as described previously (Fukushima et al., 2000). Briefly, haploid parental strains were grown on YPD plates at 30°C and cells were mated and sporulated on ME plates at 28°C (zygotic meiosis). After 1 day of incubation, the spores were separated by a micromanipulator (Singer Instruments, UK). To examine the frequency of crossing over, we measured the genetic distance (in centiMorgans) between *leu1*$^+$ and *his2*$^+$, and between *lys3*$^+$ and *cdc12*$^+$. Genetic distance was calculated according to the formula $50\times[T+(6\times NPD)]+(PD+T+NPD)$ (Perkins, 1949), where *T*, *NPD* and *PD* indicate the number of tetratypes, nonparental ditypes and parental ditypes, respectively.

Intragenic recombination rate and spore viability were determined as described previously (Shimada et al., 2002). Briefly, haploid parental strains were grown on YPD plates at 33°C. Cells were mated and sporulated on ME plates at 28°C (zygotic meiosis). After 3-4 days of incubation, spores were treated with 1% glusulase (NEN Life Science Products) for 2-3 hours at room temperature and checked under a microscope for complete digestion of contaminating vegetative cells. The glusulase-treated spores were then washed with water and used to measure the intragenic recombination rate and in the spore-viability assays. To examine the frequency of intragenic or ectopic recombination (or prototroph frequency), we used two *ade6* alleles – *ade6-M26* and *ade6-469* (Gutz, 1971) or *ade6-M26* and z7 (*ade6-469*) (Virgin and Bailey, 1998), because the reciprocal recombination between these alleles produces the *ade6*$^+$ allele.

Fluorescent microscopic observations

Cells from a single colony were cultured at 28°C in 10 ml EMM2 plus supplements [adenine (75 μg/ml), histidine (75 μ/ml), leucine (250

Table 1. Strains used in this study

Strain	Genotype	Source†
CD16-1	*h⁺/h⁻ ade6-M210/ade6-M216 cyh1/⁺ ⁺/lys5-391*	C. Shimoda (Osaka City University, Osaka, Japan)
CD16-5	*h⁻/h⁻ ade6-M210/ade6-M216 cyh1/⁺ ⁺/lys5-391*	C. Shimoda
ST194	*h⁻/h⁻ ade6-M216/210 leu1-32/leu1-32 mcp6::[mcp6-GFP-3'UTR-Lys3⁺]/mcp6::[mcp6-GFP-3'UTR-Lys3⁺] pat1-114/pat1-114*	
ST142	*h⁹⁰ ade6-M216 leu1-32 ura4-D18 mcp6::[mcp6-GFP-3'UTR-Lys3⁺] dsRed-Sad1 [::LEU2]*	
JZ670	*h⁻/h⁻ ade6-M210/ade6-M216 leu1-32/leu1-32 pat1-114/pat1-114*	M. Yamamoto (University of Tokyo, Tokyo, Japan)
TT405	*h⁻/h⁻ ade6-M216/210 leu1-32/leu1-32 ura4-D18/ura4-D18 mcp6::ura4⁺/mcp6::ura4⁺ pat1-114/pat1-114*	
CT026-1*	*h⁹⁰ leu1-32 ura4-D18 TB19::GFP-lys1⁺*	Y. Hiraoka (Kansai Advanced Research Center, Kobe, Japan)
ST193*	*h⁹⁰ leu1-32 ura4-D18 mcp6::ura4⁺ TB19::GFP-lys1⁺*	
AY174-7B	*h⁹⁰ leu1-32 ura4-D18 ade6-M210 his7::lacI-GFP-NLS-his7⁺ lys1::lacOr-lys1⁺*	K. Nabeshima (Stanford University, Stanford, CA) and A. Yamamoto (Kansai Advanced Research Center, Kobe, Japan)
ST197	*h⁹⁰ leu1-32 ura4-D18 mcp6::ura4⁺ his7::lacI-GFP-NLS-his7⁺ lys1::lacOr-lys1⁺*	
TT8-1	*h⁻ ura4⁺*	
NP32-2A	*h⁺ leu1-32 his2 ura4-D18*	Nabeshiwa et al., 2001
TT232-1	*h⁺ his2 leu1-32 ura4-D18 lys3 cdc12*	
MS105-1B	*h⁻ ade6-M26 ura4-D18*	Shimada et al., 2002
MS111w1	*h⁺ ade6-469 ura4-D18 leu1-32 his2*	Shimada et al., 2002
GP1123	*h⁺ ade6-D1 ura4-D18 leu1-32 zzz7::[ade6-469 ura4⁺]*	G. Smith
TT398	*h⁻ ura4-D18 mcp6::ura4⁺*	
TT399	*h⁺ his2 leu1-32 ura4-D18 mcp6::ura4⁺*	
TT411	*h⁻ ura4-D18 mcp6::ura4⁺ cdc12 lys3*	
TT400	*h⁻ ade6-M26 ura4-D18 mcp6::ura4⁺*	
TT401	*h⁺ ade6-469 his2 leu1-32 ura4-D18 mcp6::ura4⁺*	
TT1014	*h⁺ ade6-D1 leu1-32 ura4-D18 mcp6::ura4⁺ zzz7::[ade6-469 ura4⁺]*	
TP4-5A	*h⁻ ade6-M210 ura4-D18 leu1-32*	C. Shimoda
TP4-1D	*h⁺ ade6-M216 his2 leu1-32 ura4-D18*	C. Shimoda
TT397-5A	*h⁻ ade6-M210 leu1-32 ura4-D18 mcp6::ura4⁺*	
TT397-1D	*h⁺ ade6-M216 his2 leu1-32 ura4-D18 mcp6::ura4⁺*	
CRL790	*h⁹⁰ ade6-216 leu1-32 ura4-D18 lys1 dsRed-Sad1 [::LEU2]*	Y. Hiraoka
ST148	*h⁹⁰ ade6-M216 leu1-32 ura4-D18 mcp6::ura4⁺ dsRed-Sad1[::LEU2]*	
ST176	*h⁹⁰ leu1-32 ura4-D18(or⁺) dsRed-sad1[::LEU2] spo15-GFP::LEU2*	
ST171-1	*h⁹⁰ ade6-M210 leu1-32 ura4-D18(or⁺) mcp6::ura4⁺ dsRed-sad1[::LEU2] spo15-GFP::LEU2*	
ST191-1	*h⁹⁰ leu1-32(or⁺) dsRed-sad1[::LEU2] kms1::GFP::Kanr*	
ST172-1	*h⁹⁰ ura4-D18(or⁺) mcp6::ura4+ dsRed-sad1[::LEU2] kms1::GFP::Kanr*	
ST178	*h⁹⁰ ade6-M216 leu1-32(or⁺) ura4-D18(or⁺) dsRed-sad1[::LEU2] Taz1::GFP::Kanr*	
ST173	*h⁹⁰ ade6-M216 ura4-D18(or⁺) mcp6::ura4⁺ dsRed-sad1[::LEU2] Taz1::GFP::Kanr*	
ST179-1	*h⁹⁰ leu1-32 ura4-D18 dsRed-sad1[::LEU2] swi6⁺::GFP:leu2*	
ST174	*h⁹⁰ leu1-32 ura4-D18 mcp6::ura4⁺ dsRed-sad1[::LEU2] swi6⁺::GFP:leu2*	
YY105	*h⁹⁰ leu1-32 ura4-D18 lys1::nmt1pGFP-alpha2tubulin*	Y. Hiraoka
ST146	*h⁹⁰ leu1-32 ura4-D18 mcp6::ura4⁺ lys1::nmt1pGFP-alpha2tubulin*	
ST134	*h⁹⁰ ade6-M210 leu1-32 ura4-D18 mcp6::[mcp6-GFP-3'UTR-Lys3⁺]*	
ST196-1	*h⁹⁰ ade6-M210 leu1-32 dhc1-d3[LEU2] mcp6::[mcp6-GFP-3'UTR-Lys3⁺] dsRed-Sad1[::LEU2]*	
ST200	*h⁹⁰ ade6-M210 leu1-32 ura4-D18 taz1::ura4⁺ mcp6::[mcp6-GFP-3'UTR-Lys3⁺]*	

*TB19 signifies the N-terminal portion of DNA polymerase α (Ding et al., 2000).
†Unattributed strains were constructed for this study.

μg/ml), lysine (75 μg/ml) and uracil (75 μ/ml)] until they reached mid-log phase. The cells were collected by centrifugation, washed three times with 1 ml EMM2-N and then induced to enter meiosis by incubation in EMM2-N at 28°C for 6 hours. For live observations, we added 0.5 μg ml^{-1} Hoechst 33342 to 200 μl of the cells and an aliquot was observed under a fluorescence microscope (Olympus BX51).

For methanol fixation, cells were collected by aspiration through a glass filter (particle retention 1.2 μm; Whatman, Brentford, UK) that traps cells. The cells were then immediately immersed into methanol at −80°C and left overnight to fix the cells. The cells were then washed off the glass filter with distilled water and collected by centrifugation (2000 ***g***, 5 minutes), and the pellet was washed three times with PBS. 0.5 μg ml^{-1} Hoechst 33342 was added and the cells were observed under a fluorescence microscope.

For time-lapse observations, cells expressing GFP-tagged DNA polymerase α (Polα) (ST193 and CRL026-1) or cells expressing LacI-NLS-GFP and integrated LacO repeat at *lys1* locus (ST197 and AY174-7B) were cultured in 10 ml EMM2 plus supplements until they reached mid-log phase at 28°C. They were then induced to enter meiosis by incubation in EMM2-N at 28°C. After 5 hours of nitrogen starvation, the cells were put on a glass-bottomed dish whose surface was coated with 0.2% concanavalin A and images under a fluorescence microscope (Olympus IX71) were recorded every 2.5 minutes (1 second of exposure time) after the initiation of karyogamy. For observation of LacI-GFP dots, images were taken with a 0.3 second exposure at 5 minute intervals, with ten optical sections made at 0.5 μm intervals for each time point. Projected images obtained with Meta Morph software were analysed.

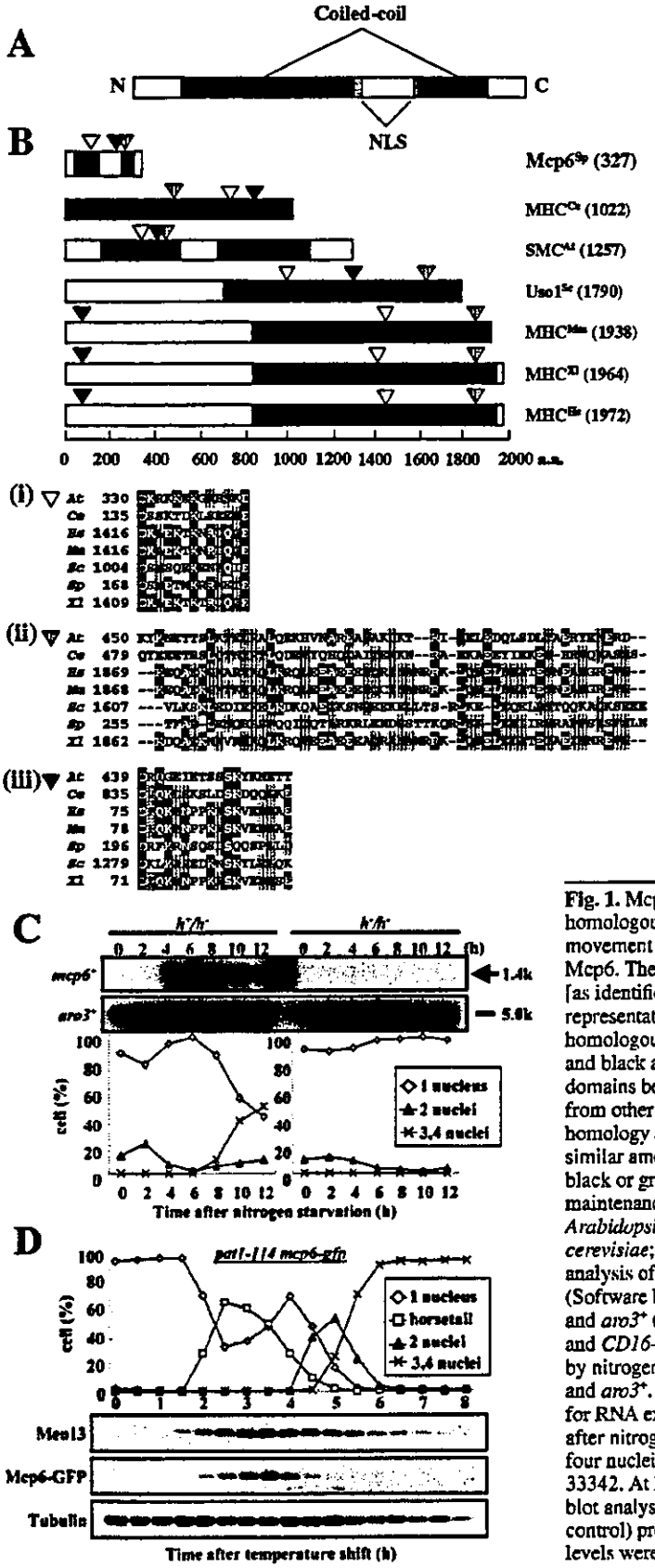

Immunofluorescence

Cells were fixed following the procedure of Hagan and Hyams (Hagan and Hyams, 1988) using glutaraldehyde and paraformaldehyde. In indirect immunofluorescence microscopy (Hagan and Yanagida, 1995), the SPB was stained with the anti-Sad1 antibody (a gift from O. Niwa, Kazusa DNA Research Institute, Kisatazu, Japan), microtubules were stained with the anti-α-tubulin antibody (TAT1). Subsequently, we added an Alexa-488-conjugated goat anti-mouse antibody (Molecular Probes, Eugene, OR) to label TAT1 or an Alexa-594-conjugated goat anti-rabbit antibody (Molecular Probes, Eugene, OR) to label anti-Sad1 antibody. The samples were then stained with 0.2 mg ml^{-1} Hoechst 33342 in PBS for 1 minute and mounted with antifade mounting medium containing 10 mg/ml *p*-phenylendiamine in 100 mM Tris-HCl (pH 8.8). Fluorescence images of these cells were observed using a fluorescence microscope (Olympus BX51) with a Cool SNAP CCD camera (Roper Scientific, San Diego, CA). Immunofluorescence images were acquired using Adobe Photoshop 7.0.

Results

Mcp6 is an *S.-pombe*-specific coiled-coil protein

Meu13 harbours a coiled-coil motif and plays a pivotal role in homologous pairing, meiotic recombination at meiosis I (Nabeshima et al., 2001) and the meiotic recombination checkpoint (Shimada et al., 2002). To identify a meiosis-specific coiled-coil protein of *S. pombe* that might interact with Meu13, we searched the genome database for uncharacterized genes that harbour coiled-coil motifs (http://www.sanger.ac.uk/Projects/S_pombe/) and found 60 genes. We then obtained DNA fragments from each of these genes and used them as probes for time-course northern blot analysis to examine their meiosis-specific

Fig. 1. Mcp6 is a meiosis-specific coiled-coil protein that harbours three homologous regions conserved in other proteins that are involved in the movement of subcellular components. (A) Schematic representation of Mcp6. The locations of the two coiled-coil motifs and the NLSs are indicated [as identified by PSORT II (http://psort.nibb.ac.jp/)]. (B) Schematic representation of Mcp6-related proteins of other species. The locations of homologous domains in these proteins are denoted by vertical white, grey and black arrowheads. Multiple sequence alignment shows homologous domains between Mcp6 from *S. pombe* (denoted *Sp*) and the related proteins from other species. Gaps inserted in the alignment to attain maximal homology are indicated by hyphens. The amino acids that are identical or similar among four or more of the seven species examined are shaded in black or grey. Abbreviations: MHC, myosin heavy chain; SMC, structural maintenance of chromosomes; Sp, *Schizosaccharomyces pombe*; At, *Arabidopsis thaliana*; Ce, *Caenorhabditis elegans*; Sc, *Saccharomyces cerevisiae*; Mm, *Mus musculus*; Xl, *Xenopus laevis*; Hs, *Homo sapiens*. The analysis of DNA sequences was performed by using the GENETYX program (Software Development, Tokyo, Japan). (C) Northern blot analysis of *mcp6*$^+$ and *aro3*$^+$ (loading control). Total RNA was extracted from *CD16-1* (h^+/h^+) and *CD16-5* (h^-/h^-) cells at the indicated times after the induction of meiosis by nitrogen starvation. RNA was blotted and probed with the ORFs of *mcp6*$^+$ and *aro3*$^+$. The graph below indicates the meiotic profiles of the cells used for RNA extraction. The progression of meiosis was monitored every 2 hours after nitrogen starvation. The numbers of cells that bear one, two, three or four nuclei were assessed by counting the nuclei stained with Hoechst 33342. At least 200 cells were counted under the microscope. (D) Western blot analysis of the production of Mcp6-GFP and Meu13 (meiotic timing control) proteins during the synchronous meiosis of strain ST194. Tubulin levels were also examined as a loading control.

transcription. This analysis identified seven novel *mcp* genes (Saito et al., 2004): *mcp1*$^+$ (AB189991); *mcp2*$^+$ (AB189990); *mcp3*$^+$ (AB189989); *mcp4*$^+$ (AB189988); *mcp5*$^+$ (AB189987); *mcp6*$^+$ (AB189986); *mcp7*$^+$ (AB189985).

Mcp6 consists of 327 amino acids and harbours two putative coiled-coil motifs, a leucine zipper (LZ), a nuclear localization signal (NLS), a peroxisomal targeting signal (PTS) and four potential Rad3-kinase phosphorylation target sites (SQ/TQ motifs) (Fig. 1A). Homology searches using the BLAST algorithm (at http://www.ncbi.nlm.nih.gov/BLAST/) indicate that Mcp6 is specific to *S. pombe*, because orthologues were not found in other organisms. Homology searching using the Block Maker program (http://bioinformatics.weizmann.ac.il/blocks/blockmkr/www/make_blocks.html) revealed that not only the coiled-coil domains but also other regions (depicted by filled vertical arrowheads) of Mcp6 are partly homologous to the myosin heavy chain (MHC), which is essential for cytokinesis (Rajagopalan et al., 2003) (Fig. 1B). Partial homology was also found with the SMC family of proteins, which are core components of the cohesin and condensin complexes that are required for chromosome movement (Jessberger, 2002). Moreover, we detected homology to Uso1, a protein required for endoplasmic-reticulum-to-Golgi vesicular transport in *Saccharomyces cerevisiae* (Sapperstein et al., 1996). A common functional feature of these proteins is their involvement in the dynamic movement of subcellular components. This suggests that Mcp6 might also be involved in subcellular dynamics.

The *mcp6*$^+$ gene is meiosis specific and expressed at the horsetail phase

To examine the meiosis-specific transcription of *mcp6*$^+$, we performed northern blot analyses of RNA obtained from CD16-1 (h^+/h^-) and CD16-5 (h^-/h^-) cells harvested at various times after the induction of meiosis by nitrogen starvation. In this experiment, we took advantage of the fact that the heterozygous CD16-1 strain initiates meiosis upon nitrogen starvation, whereas the homozygous CD16-5 strain does not. This analysis revealed that *mcp6*$^+$ displays meiosis-specific transcription that peaks at the horsetail phase (6 hours after induction), which is when homologous chromosome pairing and recombination occur (Fig. 1C).

When the Mcp6 protein appears during meiosis was then assessed by western blot analysis. To attain synchronous meiosis, we used the *pat1-114* temperature-sensitive strain, which enters meiosis in a highly synchronous manner when it is shifted to the restrictive temperature (Iino and Yamamoto, 1985). Thus, *pat1-114 mcp6*$^+$*-gfp* diploid cells that express Mcp6 protein tagged with GFP were induced to enter synchronized meiosis and their lysates were subjected to western blot analysis with an anti-GFP antibody. As shown in Fig. 1D, the frequency of horsetail nuclei is at a normal level, like the *pat1* control (Fig. 3A). Thus, we judged that the function of Mcp6-GFP is intact in this strain. Mcp6-GFP first appeared at the horsetail phase and its expression peaked at 3.5 hours after nitrogen starvation. This is similar to the timing of the production of Meu13 (Nabeshima et al., 2001). These results indicate that Mcp6 is a meiosis-specific protein that is exclusively expressed at the horsetail phase.

Mcp6 localizes to the SPB

We first examined the subcellular localization of Mcp6 by constructing a Mcp6-GFP-expressing strain in the h^{90} genetic background and inducing it to undergo meiosis by nitrogen starvation. As shown in the fluorescent microscope images in Fig. 2A (top), no GFP signal was detected during mitosis. Upon mating, however, the Mcp6-GFP fusion protein appeared as a dot near the edge of the nucleus during the horsetail period of meiosis (Fig. 2A, rows 2,

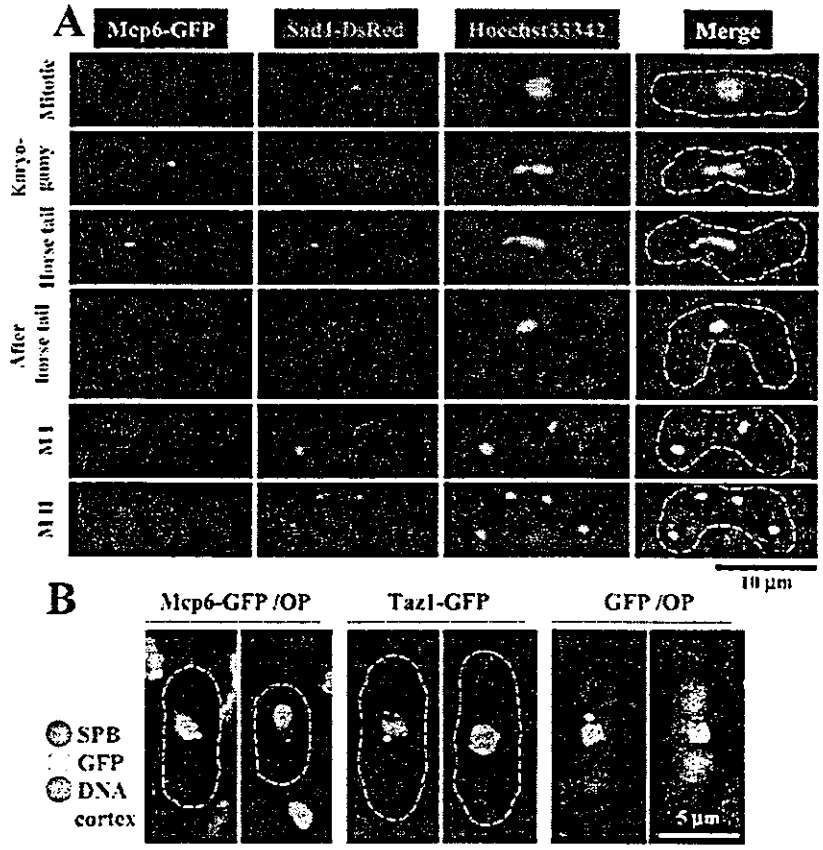

Fig. 2. Mcp6 is a meiosis-specific SPB-associated protein. (A) Microscopic analysis of Mcp6 localization during meiosis. The *mcp6*$^+$*-gfp dsred-sad1*$^+$ strain (ST142) was induced to enter meiosis by nitrogen starvation. After 6 hours of incubation, the cells were collected and fixed with methanol for microscopic observation. The GFP signal is green, the DsRed signal is red and Hoechst 33342 staining is blue. (B) Mcp6-GFP localizes to the SPB but not to the telomeres in mitotic cells. Overproduction by transforming mitotic cells with the pRGT81 (GFP expression vector) or *mcp6*$^+$/pRGT81 (Mcp6-GFP expression vector) plasmid is indicated by 'OP'.

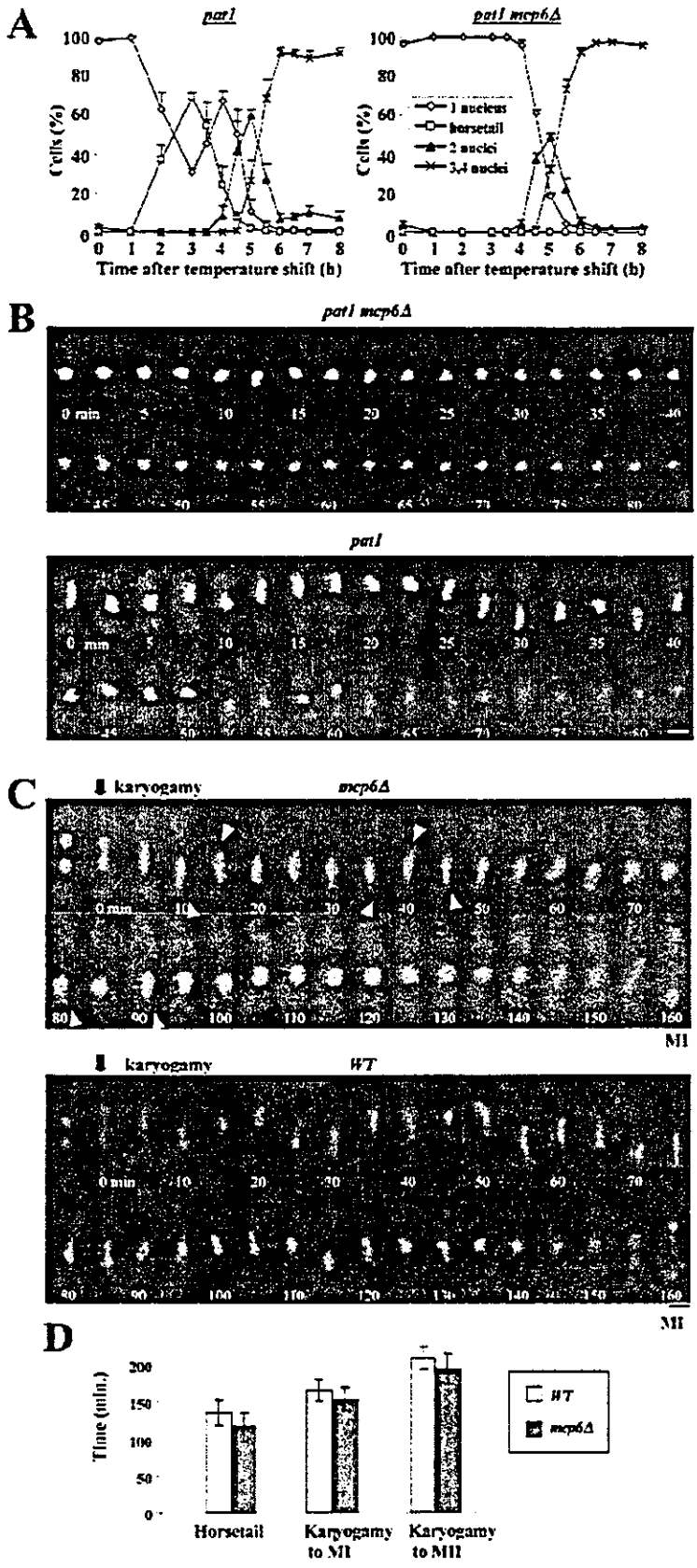

3). The dot disappeared after the horsetail period and the signal was not detected at meiosis I (MI) or meiosis II (MII). The dot localized with the fluorescence signal of Sad1-DsRed, which is known to localize to the SPB (Fig. 2A). Thus, Mcp6 is expressed only during the horsetail period of meiosis and might localize to the SPB.

Because the SPB and telomeres colocalize at this stage of meiosis, it was not clear whether Mcp6 localizes to the SPB or the telomeres. Thus, we expressed Mcp6-GFP (from the *nmt1* promoter in an expression vector pRGT81) and Sad1-DsRed (from the native promoter of *sad1*$^{+}$) during mitotic growth, which is when the SPB and telomeres localize to distinct subcellular loci. We confirmed that Sad1-DsRed does not localize with GFP-tagged Taz1, a component of telomeres, during mitosis (Fig. 2B). However, all of the Mcp6-GFP and Sad1-DsRed colocalized to the edge of the nucleus of the mitotic cells (Fig. 2B), which is where the SPB is known to be located. These results indicate that Mcp6 localizes to the SPB.

Nuclear movement during the meiotic prophase is hampered in the *mcp6Δ* mutant

To determine the role that Mcp6 plays in meiosis, we first examined the meiotic progression of *mcp6Δ* cells. To attain synchronous meiosis, we used the *pat1-114* temperature-sensitive strain again. Thus, homozygous

Fig. 3. Nuclear movement is abnormal during the horsetail phase in *mcp6Δ* cells. (A) Profiles of the meiotic progression in *pat1* (JZ670) and *pat1 mcp6Δ* (TT405) diploid cells (azygotic meiosis). The progression of meiosis was monitored every 30 minutes (3-7 hours) or 1 hour (0-2 hours and 7-8 hours) after the temperature shift, depending on the phase of meiosis. At least 200 cells were counted under a microscope to assess the frequencies of Hoechst-33342-stained cells that bear a horsetail, one nucleus, two nuclei and more than three nuclei. Each point denotes the average value of at least three independent experiments. Standard deviations are indicated as error bars. (B) Time-lapse images of *pat1* and *pat1 mcp6Δ* diploid cells during meiosis I. The nuclei were stained with Hoechst 33342. Images of a single cell were obtained at 2.5-minute intervals. The numbers at the bottom of each photograph represent the timing in minutes, with 0 minute being 2 hours after temperature shift to induce azygotic meiosis. Bar, 5 μm. (C) Time-lapse observation of wild-type (WT) (CT026-1) and *mcp6Δ* (ST193) cells during meiosis I. The nuclei were visualized by the fluorescence of a Polα-GFP fusion construct. Images of a single cell were obtained at 5 minute intervals. The numbers at the bottom of each photograph represent the timing in minutes, with 0 minutes being when nuclear fusion (karyogamy) occurs. The white arrowheads indicate the putative trailing edge of the moving nucleus. Bar, 5 μm. (D) The duration of meiotic prophase, meiosis I (MI) and meiosis II (MII) in *mcp6Δ* and WT cells. The average values were calculated from ten independent cells observed under a microscope. Standard deviations are shown as error bars.

diploid *pat1-114* cells were arrested at the G_1 phase by nitrogen starvation and then shifted to the restrictive temperature to induce synchronous meiosis. We then observed over time the number of nuclei in the cells of the *pat1-114* strain, whose *mcp6*$^+$ gene is intact, and in the cells of the *pat1-114 mcp6Δ* mutant. We found that the times at which cells with two or four nuclei peaked were similar for both strains (Fig. 3A).

Notably, almost no *pat1-114 mcp6Δ* cells (<0.5%) displayed the flat nuclear shape or the non-central position of the nucleus that are characteristic of the horsetail period. This is reminiscent of the description of the cells that bear a mutation in the SBP component Kms1 – that the nuclear shapes of these cells at prophase I of meiosis were aberrant (Shimanuki et al., 1997). Because the oscillatory nuclear movement that normally occurs during the prophase in wild-type meiosis (Chikashige et al., 1994) is impaired in the *kms1-null* mutant (Niwa et al., 2000), we surmised that deletion of *mcp6*$^+$ would also abolish nuclear migration. Thus, we examined over time the movement of chromosomes in *pat1-114 mcp6Δ* cells under a microscope. We found that horsetail oscillation at the prophase of meiosis I was indeed abrogated in these cells (Fig. 3B, top). In fact, almost no nuclear movement was observed throughout the prophase of meiosis in any of the *pat1-114 mcp6Δ* cells that we examined. By contrast, *pat1-114* cells displayed the marked nuclear oscillations that characterize this meiotic period (Fig. 3B, bottom).

Because the effects of mating and karyogamy cannot be observed at the restrictive temperature in the azygotic meiosis of *h*$^-$/*h*$^-$ *pat1-114* homozygous diploid cells, we also assessed the effect on nuclear oscillation of deleting the *mcp6*$^+$ gene in the h^{90} genetic background. Thus, we subjected these cells expressing Polα-GFP to time-lapse observation under a microscope. As shown in Fig. 3C (top), it is apparent that nuclear oscillation at prophase of meiosis I is also impaired in *mcp6Δ* cells. Notably, in contrast to *pat1-114 mcp6Δ* cells, slight movement was observed just after karyogamy, although no apparent movement was detected thereafter. The nucleus does seem to be moving a little in *mcp6Δ* cells because a trace of the trailing edge of the moving nucleus can be observed (Fig. 3B, white arrowheads). Nonetheless, it is evident that chromosomal movement is largely hampered in *mcp6Δ* cells compared with the vigorous nuclear movements in wild-type cells that occur several times after karyogamy (Fig. 3C, bottom).

Although it seems that the horsetail period (117 minutes) and the periods from karyogamy to meiosis I (154 minutes) and from karyogamy to meiosis II (195 minutes) in *mcp6Δ* cells were slightly shorter than those of wild-type cells (136 minutes, 166 minutes and 209 minutes, respectively) (Fig. 3D), these changes were not statistically

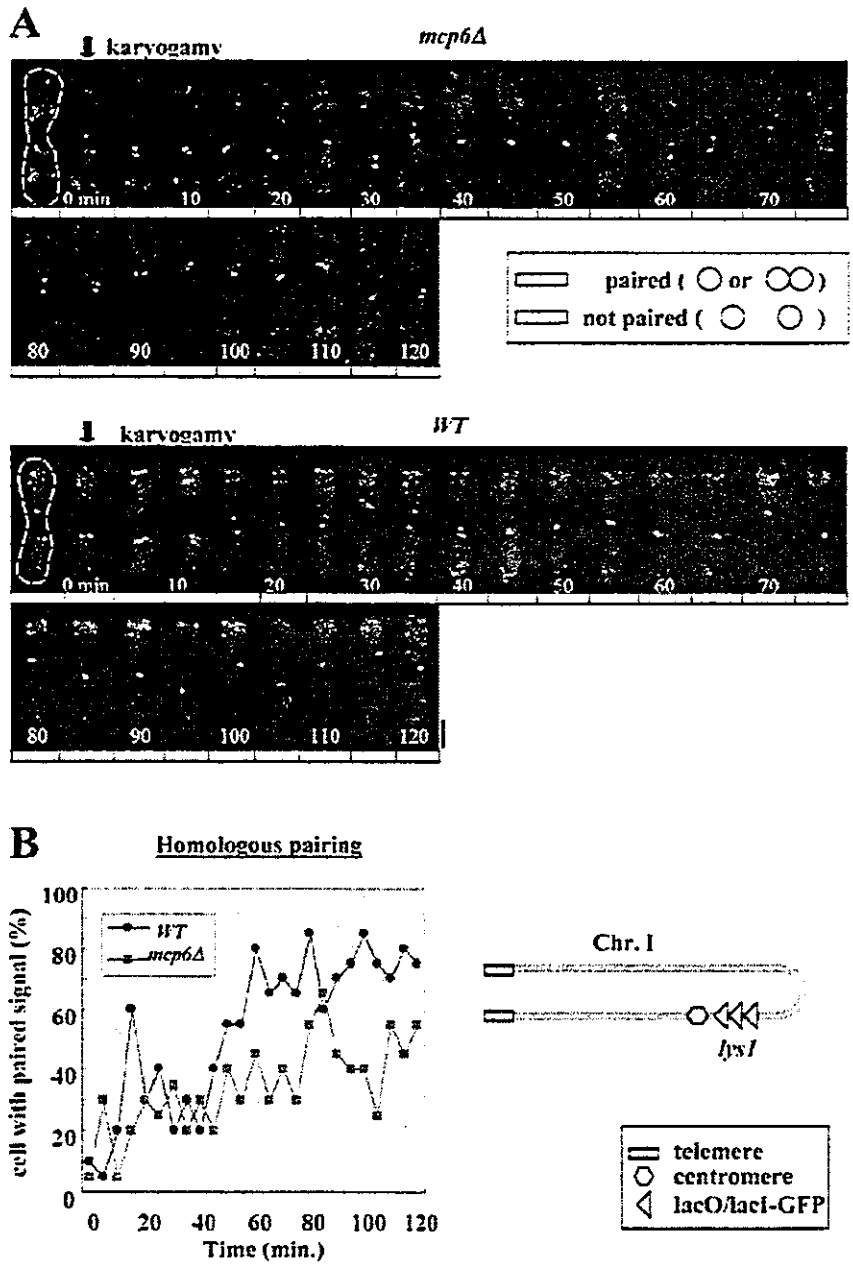

Fig. 4. Homologous pairing is reduced in *mcp6Δ* cells. (A) Time-lapse observation of the *lys1* locus in a living cell, either *mcp6Δ* (ST197) or wild type (WT) (AY174-7B), during the horsetail stage. The *lacO* repeat sequence integrated into the *lys1* loci was visualized by the LacI-NLS-GFP fusion protein. Images of a single cell were obtained at 5 minute intervals. The numbers at the bottom of each photograph represent the timing in minutes, with 0 minutes being when nuclear fusion (karyogamy) occurs. The rectangles under each photo indicate that the *lys1* loci were paired (grey) or not paired (white). Bar, 5 μm. (B) Time course of homologous pairing frequency during the horsetail stage in *mcp6Δ* (red square) compared with that in the WT (blue circle). The average values were calculated from 20 independent cells. The *lys1* locus in chromosome I is illustrated as an inset.

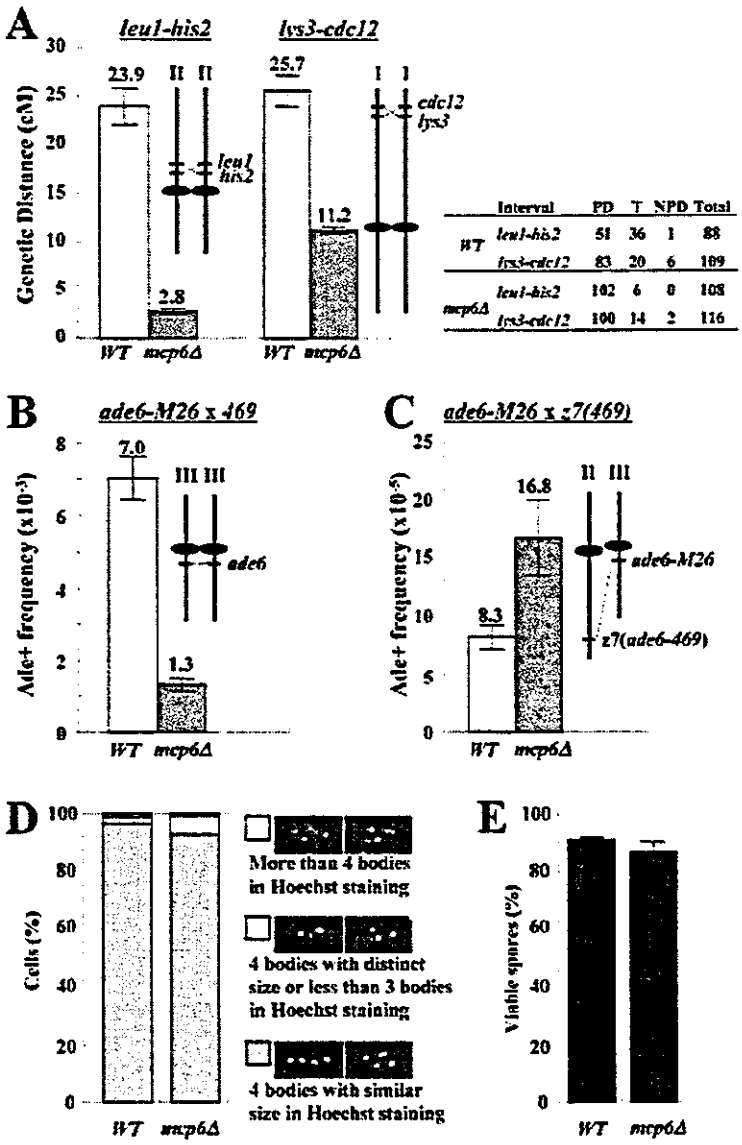

Fig. 5. Homologous recombination is reduced in *mcp6Δ* cells but ectopic recombination is increased compared with wild-type (WT) cells. The chromosomal positions of the loci and centromeres are illustrated in the insets. (A) Intergenic recombination (crossing over) showing the intervals between *leu1* and *his2* (left), *lys3* and *cdc12* (middle) and the primary tetrad (right). Only those tetrads that generated four viable spores were used to calculate the genetic distances (cM). The strains examined for *leu1-his2* crossing were WT (TT8-1 × NP32-2A) and *mcp6Δ* (TT398 × TT399), whereas the strains used for the *lys3-cdc12* crossing were WT (TT8-1 × TT231-1) and *mcp6Δ* (TT399 × TT411). The data shown are the average values calculated from at least three independent assays (at least 40 tetrads were dissected per assay). (B) Intragenic recombination. The strains examined were WT (MS105-1B × MS111w1) and *mcp6Δ* (TT400 × TT401). The average values were calculated from at least three independent assays. (C) Ectopic intragenic recombination. The strains crossed were WT (MS105-1B × GP1123) and *mcp6Δ* (TT400 × TT1014). The average values were calculated from at least three independent assays. Standard deviations are indicated as error bars. (D) Spores of *mcp6Δ* cells are almost normal as judged by the frequency of abnormal ascospores. The haploid parental strains were mated and sporulated on ME plate. After overnight culture, the cells were fixed with 70% ethanol for staining with Hoechst 33342. At least 200 cells were counted. (E) Spore viability of WT (TP4-5A × TP4-1D) and *mcp6Δ* (TT397-5A × TT397-1D) cells. Random spore analysis was performed.

significant ($P>0.05$ in Student's *t*-test). Thus, we conclude that the durations of the horsetail period, meiosis I and meiosis II are almost normal in h^{90} *mcp6Δ* cells (zygotic meiosis), as they are in the *pat1-114* genetic background (azygotic meiosis).

Homologous pairing is reduced in *mcp6Δ* cells

To investigate the requirement of Mcp6 in the process of chromosome pairing, we observed the homologous chromosomal regions in living zygotes during horsetail phase. By integrating a tandem repeat of the *Escherichia coli lac* operator sequence into the *S. pombe* genome at the *lys1*$^+$ locus (near the centromere of chromosome I), the fusion gene encoding GFP-LacI-NLS (which binds to the *lac* operator) was expressed in this strain. Consequently, two homologous loci on the chromosomes were visualized with GFP fluorescence (Nabeshima et al., 2001). In wild-type background, these homologous loci repeatedly associated and dissociated in the horsetail nucleus, oscillating back and forth between the cell poles (Fig. 4A, bottom). By contrast, the paired GFP signals were less frequent in *mcp6Δ* cells than in wild-type cells (Fig. 4A, top).

In order to quantify the pairing activity during the horsetail phase, we scored the occurrence of paired signals every 5 minutes from karyogamy to the first meiotic nuclear division in 20 live individuals of each strain. In the wild-type strain, the population of cells with paired signals during the initial 45 minutes was about 30% and then increased to about 80%. This level was maintained until 120 minutes (Fig. 4B, blue line). In *mcp6Δ* cells, there was no significant difference from the wild type in the initial 45 minutes but the subsequent increase in pairing observed in the wild type was completely absent (Fig. 4B, red line). These results indicate that Mcp6 is required for promoting homologous pairing with horsetail movement.

Meiotic recombination is abnormal in *mcp6Δ* cells

To determine whether, like the other SPB component Kms1, Mcp6 plays a role in meiotic recombination (Niwa et al., 2000), we compared the rates of intergenic and intragenic recombination in *mcp6Δ* and wild-type strains. We first investigated the crossover recombination of zygotic meiosis by tetrad analysis, which allowed us to measure the genetic distance between *leu1* and *his2* (Fig. 5A, insets). When the *mcp6Δ* strain was crossed, the genetic distance between *leu1* and *his2* was only 12% of the distance obtained when the wild-type strain was crossed (Fig. 5A, left). The genetic distances

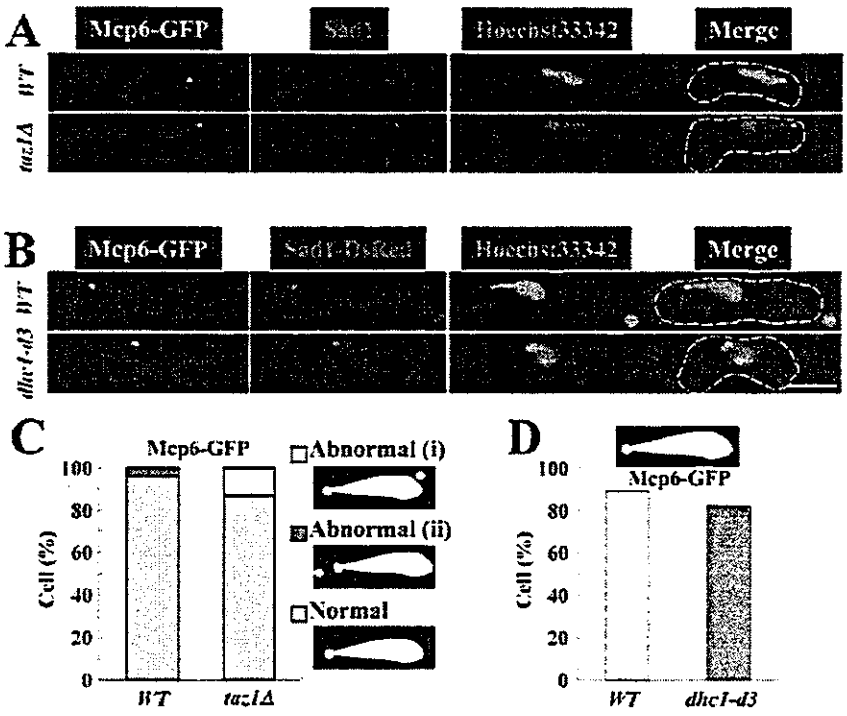

Fig. 6. The localization of Mcp6-GFP is normal in *taz1Δ* and *dhc1-d3* cells. (A) A typical immunofluorescence image of Mcp6-GFP at the horsetail phase in wild type (ST134) and *taz1Δ* (ST200) cells. (B) A typical image of Mcp6-GFP at the horsetail phase in wild-type (ST142) and *dhc1-d3* (ST196) cells (living). Bar, 5 μm. (C) Frequency of cells in which the Mcp6-GFP signals localize with Sad1 to the leading edge of the horsetail nucleus in the wild type and *taz1Δ* cells. (D) Frequency of cells in which the Mcp6-GFP signals localize with Sad1-DsRed to the leading edge of the horsetail nucleus in the wild-type and *dhc1-d3* cells.

between *lys3* and *cdc12* in the *mcp6Δ* strain was also reduced to 44% of that observed in the wild-type strain (Fig. 5A, right). We also characterized the intragenic recombination of the *mcp6Δ* strain between two different mutant alleles of *ade6* (*M26* and *469*). When the *mcp6Δ* strain was crossed, the frequency of Ade$^+$ recombinant spores was 19% of the wild-type frequency (Fig. 5B). Thus, it appears that Mcp6 plays a significant role in meiotic recombination.

To characterize the meiotic recombination competency of the *mcp6Δ* strain further, we examined the ectopic recombination rate. We used a pair of *ade6* alleles from different chromosomal loci, one at the natural position of *ade6* on chromosome III and the other at the *pacI* locus on chromosome II (*z7*) (Virgin and Bailey, 1998) (Fig. 5C). Notably, the frequency of ectopic recombination between these two loci in *mcp6Δ* cells was twice (202%) (in the *M26* and *469* pair) that of wild-type cells (Fig. 5C). A similar increase in the ectopic recombination rate between *M26* and *z15* (telomere of chromosome I) has been reported for the *kms1Δ* strain (Niwa et al., 2000). However, *mcp6Δ* cells are distinct from *kms1Δ* cells in that they do not display the abnormal telomere clustering that characterizes *kms1Δ* cells.

When we observed the spore morphology of *mcp6Δ* cells, we found that almost all of the spores looked normal (Fig. 5D). Indeed, depletion of Mcp6 caused only about 4% of the asci to display abnormal numbers of ascospores. The spore viability is also similar to that of wild-type cells (Fig. 5E). Thus, we conclude that Mcp6 does not play an important role in spore formation.

Taz1 and Dhc1 are not required for the localization of Mcp6 at the leading edge of the horsetail nucleus

In addition to chromosome oscillation at the horsetail phase, telomere clustering is required for the alignment and subsequent association of homologous chromosome arms (Ding et al., 2004). The telomere protein Taz1, whose deletion causes G_2/M-phase DNA-damage-checkpoint delay, chromosome mis-segregation and double-stranded DNA breaks, plays a role in preventing and repairing DNA breaks (Miller and Cooper, 2003) and telomere clustering (Cooper et al., 1998). To determine whether the SPB localization of Mcp6 depends on proper telomere clustering, we prepared *taz1* null mutant cells harbouring the integrated *mcp6$^+$-gfp* gene driven by its own promoter. These cells were then induced to enter meiosis by nitrogen starvation and the Mcp6-GFP signal was observed by immunofluorescence. As shown in Fig. 6A,C, the subcellular localization of Mcp6-GFP was almost normal in *taz1Δ* cells (71 cells were counted in both wild-type and *mcp6Δ* cells).

We next examined whether SPB localization of Mcp6 is dependent on dynein. To do this, we prepared a *dhc1-d3* mutant harbouring the integrated *mcp6$^+$-gfp* gene driven by its own promoter and induced it to enter meiosis by nitrogen starvation. Mcp6-GFP colocalized normally with DsRed-Sad1 to the SPB in *dhc1-d3* cells, which suggests that Dhc1 is not required for the proper localization of Mcp6 at the SPB (Fig. 6B). The frequency of cells in which Sad1-DsRed and Mcp6-GFP colocalized to the leading edge of the horsetail nucleus was 94% (15/18) in *dhc1-d3* cells, which is almost equal to the frequency in wild-type cells (93%; 32/36) (Fig. 6D).

Subcellular localization of SPB components is normal in *mcp6Δ* cells

For proper horsetail movement, it is essential that the telomeres cluster at the SPB after karyogamy and that the telomere/SPB complex migrates on the microtubule that radially extends from the SPB to the cell cortex on the opposite site of the cell. To understand the role of Mcp6 in horsetail movement, we examined the subcellular localization of the SPB components Sad1, Spo15 and Kms1 in *mcp6Δ* cells. Sad1 is a constitutive component of SPB that is essential for normal bipolar spindle formation (Hagan and Yanagida, 1995), Spo15 is associated with SPBs throughout the life cycle and plays an indispensable role in the initiation of spore membrane formation (Ikemoto et

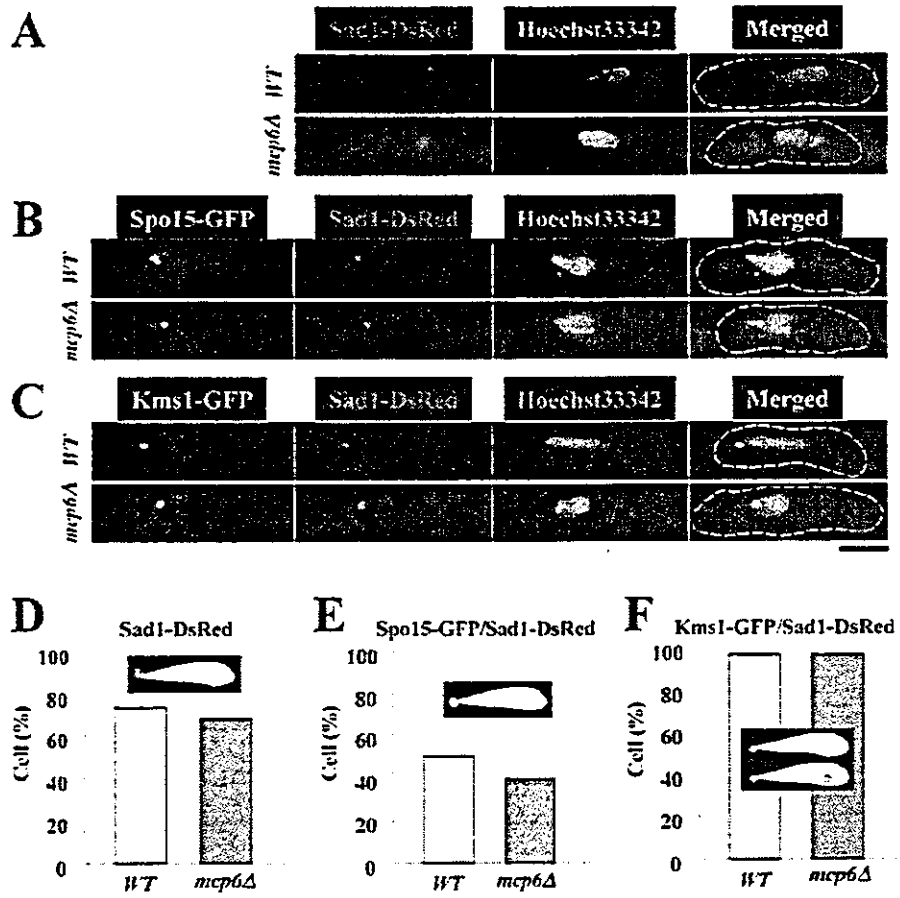

Fig. 7. The subcellular localization of GFP-tagged SPB components at the horsetail phase is normal in *mcp6Δ* cells. The h^{90} strains that express Sad1-DsRed (WT, CRL790; *mcp6Δ*, ST148) (A), Spo15-GFP (*WT*, ST176; *mcp6Δ*, ST171-1) (B) or Kms1-GFP (*WT*, ST191-1; *mcp6Δ*, ST172-1) (C) fusion proteins were induced to enter meiosis by nitrogen starvation. After 6 hours, the cells were collected and observed under a fluorescence microscope. Typical images are shown. (D) The proportions of the cell population in which Sad1-DsRed localized to the leading edge of the nucleus with a single dot, as depicted in the inset. (E) The proportions of the cell population in which Spo15-GFP and Sad1-DsRed colocalized to the leading edge of the nucleus with a single dot, as depicted in the inset. (F) The proportions of the cell population in which Kms1-GFP and Sad1-DsRed colocalized to the leading edge of the nucleus, as depicted in the inset. Green, GFP; red, Sad1-DsRed; blue, Hoechst 33342. The dotted line depicts the contour of the cell. Bar, 5 μm.

al., 2000), and Kms1 is required for the formation of meiotic prophase-specific nuclear architecture (Shimanuki et al., 1997). To do this, we prepared strains that express the Sad1-dsRed protein and the other GFP-fused components from their own promoters in the *mcp6-null* genetic background. The cells were induced to enter meiosis by nitrogen starvation and then observed under a fluorescence microscope.

We first investigated the localization of Sad1-dsRed during the horsetail phase and found that, in *mcp6Δ* cells, 68% (17/25) of the Sad1 signal constituted a single dot at the leading edge of the nucleus (Fig. 7A,D). This is similar to what is observed in wild-type cells (59/82, or 72%, of the Sad1 signal is present as a single dot). These results indicate that Mcp6 is not required for Sad1 localization to the SPB. We next examined the localization of Spo15-GFP and found that most of the Spo15 signal localized with Sad1-DsRed to the SPB in both *mcp6Δ* and wild-type cells (Fig. 7B,E). We also examined the localization of Kms1-GFP and found that most Kms1-GFP and Sad1-DsRed colocalized to either the SPB or the Sad1 body in both *mcp6Δ* and wild-type cells (Fig. 7C,F). These results indicate that Mcp6 is not required for the proper organization of SPB architecture.

Telomere localization is normal but microtubule organization is abnormal in *mcp6Δ* cells

Telomere clustering near the SPB, which occurs during the prophase of meiosis I, is an essential event for efficient chromosome pairing and cells deficient in the telomere-associated protein Taz1 (*taz1Δ*) have been reported to have defective telomere clustering, reduced recombination rates, abnormal spore formation and reduced spore viability (Nimmo et al., 1998; Cooper et al., 1998). To determine whether telomere clustering is normal in *mcp6Δ* cells, we examined the subcellular localization of the telomere proteins Taz1 and Swi6 by preparing h^{90} *taz1⁺-gfp sad1⁺-dsred* and h^{90} *swi6⁺-gfp sad1⁺-dsred* strains, which express Sad1-dsRed together with GFP-tagged Taz1 or Swi6 from their own promoters. These strains were induced to enter meiosis by nitrogen starvation and then observed under a fluorescence microscope. The Taz1-GFP signal of the telomere at the leading edge of the nucleus localized with the Sad1-DsRed signal to the SPB in 62% (23/37) and 58% (14/24) of the *mcp6Δ* and wild-type cells, respectively (Fig. 8A,D). The Swi6-GFP signal also localized with the Sad1-DsRed signal to the SPB at similar levels in *mcp6Δ* (76%; 13/17) and wild-type cells (85%; 35/41) (Fig. 8B). These results indicate that the subcellular localization of Taz1 and Swi6 is normal in *mcp6Δ* cells – namely, Mcp6 is required for neither SPB organization nor telomere clustering.

The oscillatory nuclear movement is mediated by dynamic reorganization of astral microtubules originating from the SPB. To observe the organization of microtubules in *mcp6Δ* cells, we prepared the h^{90} strain that expresses GFP-fused α-tubulin from the *nmt1* promoter. After 6 hours' induction of meiosis

in EMM2-N medium, the strain was fixed with glutaraldehyde and paraformaldehyde for immunostaining. In wild-type cells, 95% (156/165) of astral microtubules originated from the SPB during the horsetail phase. In *mcp6Δ* cells, however, collapse of astral microtubule organization was observed (Fig. 8C,F): 21% (21/100) of *mcp6Δ* cells displayed the microtubules not associated with SPB [Fig. 8F, abnormal (i)]. We also found that 60% (60/100) of *mcp6Δ* cells showed abnormal astral microtubules that originated from the SBP but branched elsewhere [Fig. 8F; abnormal (ii)]. These results indicate that Mcp6 is required for proper astral microtubule positioning during horsetail phase.

Discussion

Mcp6 is required for horsetail movement of chromosomes

In the present study, we show that Mcp6 is a novel coiled-coil protein that is only expressed during the horsetail period of meiosis (Fig. 1) and localizes to the SPB (Fig. 2). We found that the deletion of *mcp6*$^+$ almost abolished horsetail movement of chromosomes (Fig. 3) and reduced recombination rates (Fig. 5). Notably, we observed that, whereas deletion of *mcp6*$^+$ from the homozygous diploid *pat1* genetic background completely abolished horsetail movement during azygotic meiosis of these cells (Fig. 3B), a slight chromosome movement after karyogamy was observed during the zygotic meiosis of *mcp6Δ* cells in the h^{90} genetic background (Fig. 3C). This indicates that karyogamy is important for initiating horsetail movement and suggests that Mcp6 plays a role during or just after karyogamy. BLAST-based homology searches failed to identify proteins in other species that are homologous to Mcp6. Thus, Mcp6 is an *S.-pombe*-specific protein. This is reasonable because *S. pombe* is the only organism examined so far that displays horsetail movement of nucleus.

Two *S. pombe* mutants [*kms1-1* (Shimanuki et al., 1997; Niwa et al., 2000) and *dhc1* mutants (Yamamoto et al., 1999)] have been reported to lack horsetail movement. Another mutant (*dlc1Δ*) also shows abnormal horsetail movement (Miki et al., 2002). Although Kms1, which is also an *S.-pombe*-specific protein, localizes to the SPB throughout mitotic and meiotic phases, abnormal phenotypes of *kms1-1* cells are only detected in meiosis (Niwa et al., 2000). Dhc1, the dynein heavy chain that is conserved among various species, localizes to the SPB, microtubules and cell cortex, and is predominantly expressed from karyogamy through to meiosis I (Yamamoto et al., 1999). Thus, Mcp6 is a new

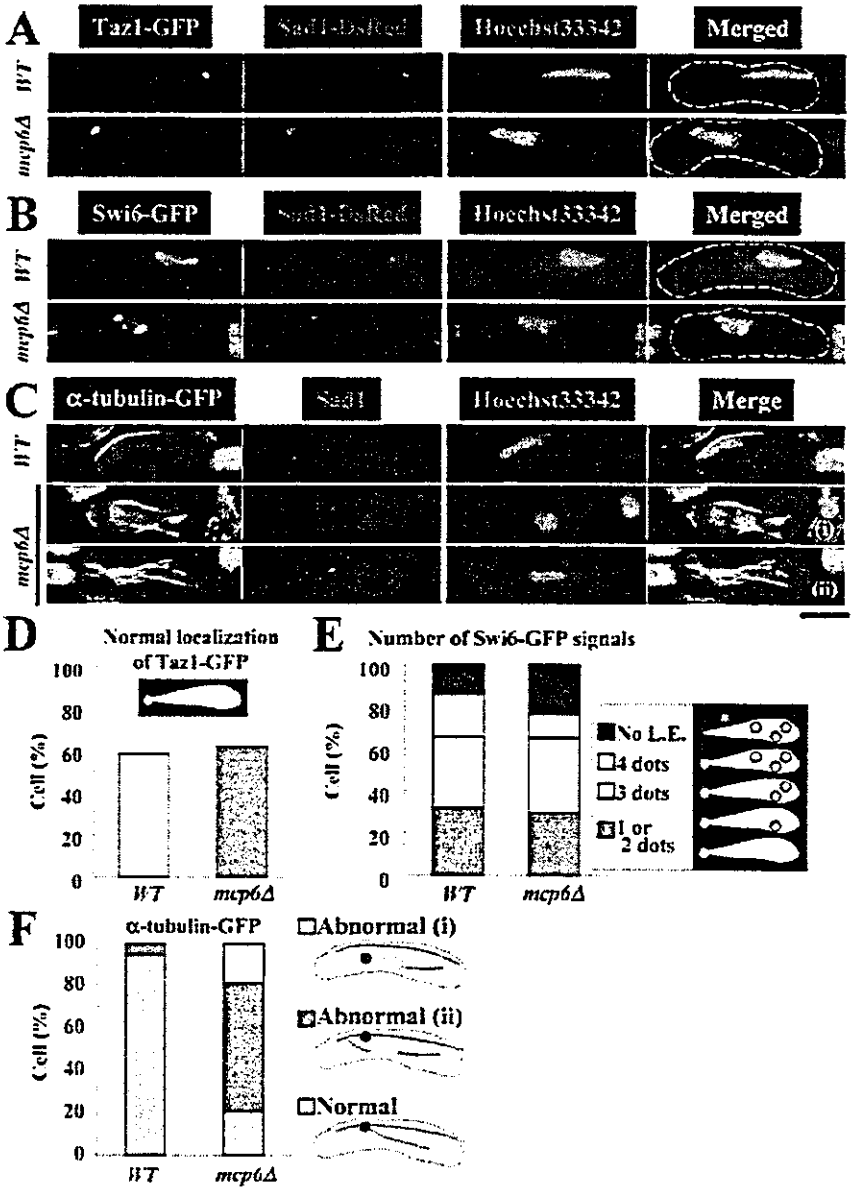

Fig. 8. GFP-tagged telomere components and α-tubulin localize normally in *mcp6Δ* cells. The h^{90} strains that express Taz1-GFP (*WT*, ST178; *mcp6Δ*, ST173) (A), Swi6-GFP (*WT*, ST179-1; *mcp6Δ*, ST174) (B) or α-tubulin-GFP (*WT*, YY105; *mcp6Δ*, ST146) (C) were induced to enter meiosis by nitrogen starvation. After 6 hours, the cells were collected and observed under a fluorescence microscope. Images shown in (C) were obtained by immunofluorescence. Typical images are shown. (D) The proportions of the cell population in which Taz1-GFP and Sad1-DsRed colocalized to the leading edge of the nucleus with a single dot, as depicted in the inset. (E) The proportions of the cell population in which Swi6-GFP and Sad1-DsRed colocalized to the leading edge (L.E.) of the nucleus with extra dots of Swi6-GFP in the nucleus, as depicted in the insets. (F) The proportions of the cell population that display normal or abnormal (i) and (ii) tubulin positioning as depicted on the right. Green, GFP; red, Sad1-DsRed (A,B) or Sad1 (C); blue, Hoechst 33342. The dotted line indicates the contour of the cell. Bar, 5 μm.